Environmental Earth Sciences (2024) 83:392
https://doi.org/10.1007/s12665-024-11618-x

ORIGINAL ARTICLE

Modeling the total hardness (TH) of groundwater in aquifers using novel hybrid soft computing optimizer models

Hossein Moayedi[1,2] · Marjan Salari[3] · Sana Abdul-Jabbar Ali[4] · Atefeh Ahmadi Dehrashid[5] · Hossein Azadi[6]

Received: 21 October 2022 / Accepted: 27 April 2024 / Published online: 12 June 2024

Abstract

A groundwater reservoir is either a solitary aquifer or a network of interconnected aquifers. A particular aquifer's groundwater purity evaluation could be time-consuming and costly. This study quantified the properties of Na%, SO_4^{2-}, Cl, Na^+, Mg^{2+}, Ca^{2+}, HCO_3^-, K^+, and pH to predict the water quality parameter known as total hardness (as $CaCO_3$). Groundwater quality data for the Shiraz Plain from 2002 to 2018 was utilized to accomplish this objective. The paper contrasts a hybrid methodology that combines Teaching Learning-Based Optimization (TLBO), Multiverse Optimizer (MVO), the Cuckoo Optimization Algorithm (COA), and the Evaporation Rate-based Water Cycle Algorithm (ER-WCA) with Artificial Neural Networks (ANN) this was done to design an optimal network for groundwater quality with conventional ANN. In comparison to all other TLBO-ANN, MVO-ANN, and COA-ANN developed models, the ER-WCA-ANN technique (with a population size of 500 and eight neurons in each hidden layer) provided the most accurate prediction for the TH with R^2 values of 0.9983 and 0.98261, and RMSE values of 0.03698 and 0.00611, respectively, in the training and testing datasets. A comparison of the findings for the forecasting of groundwater quality showed that the ER-WCA-ANN hybrid model might increase prediction accuracy. These findings may have significant implications for future groundwater quality assessments.

Keywords Groundwater quality · Machine learning · Teaching Learning-Based Optimization (TLBO) · Multiverse Optimizer (MVO) · Cuckoo Optimization Algorithm (COA)

Introduction

Increasing the demand for potable water heightens the awareness of the state of groundwater management (Salari et al. 2018). The decline in the groundwater quality induced by natural products and human endeavors in the adjacent soil could negatively affect public health if left ignored (Khudair et al. 2018; Salari et al. 2017). Understanding the factors that affect groundwater quality is necessary to determine the water's suitability in the location. However, a groundwater resource's quality depends on its natural constituents, such as sediments, bacteria, and chemical substances. The water source's pathogens and contaminants primarily affect human health (Shen et al. 2023).

The World Health Organization (WHO) has been disseminating information and revising standards and instructions

✉ Marjan Salari
salari.marjan@gmail.com; m.salari@sirjantech.ac.ir

Hossein Moayedi
hosseinmoayedi@duytan.edu.vn

Sana Abdul-Jabbar Ali
sana.a.ali@alsafwa.edu.iq

Atefeh Ahmadi Dehrashid
atefeh.ahmadi@uok.ac.ir

Hossein Azadi
hossein.azadi@uliege.be

[1] Institute of Research and Development, Duy Tan University, Da Nang 550000, Viet Nam

[2] School of Engineering and Technology, Duy Tan University, Da Nang, Viet Nam

[3] Department of Civil Engineering, Sirjan University of Technology, Sirjan, Iran

[4] Pharmacy Department, AlSafwa University College, Karbalaa, Iraq

[5] Department of Climatology, Faculty of Natural Resources, University of Kurdistan, Sanandaj, Iran

[6] Department of Economics and Rural Development, Gembloux Agro-Bio Tech, University of Liège, Gembloux, Belgium

for all contaminants and metals that may be of concern when evaluating groundwater quality (Organization 1993). The majority of the parameters that are measured in a water sample have only a limited impact on the suitability of the water for potable use, as they are unlikely for health issue when concentrations increase, whereas others may be hazardous at negligible concentrations. One of the parameters that is measured in groundwater samples that is commonly assumed to have a negligible health impact is Total Hardness (TH). TH levels below 100 mg/L as $CaCO_3$ may cause the dissolution of carbonate mineral, and TH values greater than about 200 mg/L as $CaCO_3$ may cause carbonate precipitates to form. Despite the common assumption that this parameter has no impact on human health, a number of studies have demonstrated a potential inverse relationship between the hardness value in drinking water and cardiovascular disease. Evaluation of the purity of groundwater could be an intriguing endeavor. A representative quality assessment may call for many samples, depending on a resource's size and the location of wells. The results of this research show that establishing a functional link between these easily observed characteristics and groundwater ion concentrations saves the work and time required for off-site analysis (Hanoon et al. 2022).

In water quality simulation, machine learning models have shown considerable promise because they can identify the statistical link between input and output data without explicitly knowing the physical processes. This enables a thorough investigation of the biological, hydrological, and environmental factors that affect water quality (Zhu et al. 2022). Recently, the application of artificial intelligence (AI) algorithms to hydrological studies of nitrate pollution has produced favorable outcomes. These algorithms can effectively solve intricate nonlinear problems because they gain knowledge from the dataset and do not need rules specified by experts (Gholami and Booij 2022). Additionally, it has been shown that AI algorithms improve the propensity for predicting various environmental activities (Wu et al., 2024: Moayedi et al. 2023a, b; Tyralis et al. 2019). Creating optimum functions in an artificial neural network (ANN) depends on the choice of input variables and transfer functions. A greater understanding of hydrogeological processes and behavior is necessary to manage and enhance groundwater quality efficiently. However, developing such forecasts requires employing specialist equipment due to the hydrogeological system's complex and changing properties (Nordin et al. 2021).

An ANN model, which takes its cues from how the human brain processes information, instruction, and learning, is one of these techniques. Contrarily, coupling of ANN with optimization techniques has aided the modeling of complex nonlinear hydrological systems and can assist with water resources management. As a result, many researchers are interested in the high accuracy and stability that an AI framework can provide in the modeling of complicated groundwater and surface water systems, as detailed by researchers from various disciplines (Khalid et al. 2020; Leal Filho et al. 2020 Salami et al. 2016a, b; Salami et al. 2016a, b; Salari et al. 2021; Sarker et al. 2021). The neural network theory presented by Zurada (1992) is understandable by readers with varying levels of technical instruction. Hagan et al. (1997) provide a practical description of ANN techniques in conjunction with illustrative applications. Yalcintas and Akkurt (2005) demonstrate the applicability of ANN methods to predicting building energy and energy savings due to building retrofits.

Recent years have also seen the application of several machine learning techniques, including the classification and regression tree (CART) (Naghibi et al. 2016), support vector machine (SVM) (Naghibi et al. 2017), and random forest (RF) technology (Rahmati et al. 2016). According to Khosravi et al. (2018), one advantage of machine learning algorithms is their capacity to manage vast quantities of nonlinear structured data from several sources over a range of scales. Various hydrological disciplines have employed the ANN, one of the most well-liked and commonly applied techniques (Tsakiri et al. 2018). The computational efficiency of ANNs has its benefits, but it also has drawbacks, including producing inaccurate modeling and having a poor prediction capacity (Bui et al. 2016).

Hybrid approaches are known to improve prediction accuracy because they have more prediction power and recognition capacity than single-based classifiers (Chen et al. 2019a, b). However, the outcome of the modeling process depends on both the model's ability to predict the future and the quality of the data. In light of this, the likelihood of obtaining correct findings will rise by choosing an appropriate dataset and model. Chen et al. (2019a, b) analyzed the mapping of groundwater potential in the Zhangjiamao area of China using an adaptive neuro-fuzzy inference system (ANFIS), Teaching Learning-Based Optimization (TLBO), Multiverse Optimizer (MVO), the Cuckoo Optimization Algorithm (COA), and the Evaporation Rate-based Water Cycle Algorithm (ER-WCA). To create models and carry out validation, 93 spring sites in the study area were initially chosen and then randomly divided in a ratio of 70:30. The correlation research between spring occurrences and the influencing factors was conducted using the probability certainty factor (PCF) approach. Later, GSPMs were created utilizing the ANFIS-TLBO and ANFIS-BBO models to simulate groundwater spring potential. The area under the receiver operating characteristic (AUROC) technique was used to assess the GSPMs. The analysis revealed that the ANFIS-TLBO model's training and validation dataset's AUROC scores were 0.866 and 0.905, respectively.

However, based on the training and validation datasets, the ANFIS-BBO model's AUROC scores were 0.861 and 0.887. In contrast to the predictions of the ANFIS-BBO model (30.52%), the results of ANFIS-TLBO showed that 25.66% of the research area could be classified into the high and very high groundwater spring potential classes. The findings of the present research could be helpful for groundwater management.

Another study by Sunayana et al. (2020) simulated the groundwater quality at a sanitary landfill site utilized to dispose of solid waste using artificial neural networks. The groundwater quality was assessed at ten locations nearby for two consecutive years, 2016–2017and the data were then used for modeling. Using three learning strategies, neural networks predicted TH, with the most accurate method being used in the prediction model. Interpolation maps for both years were produced using the inverse

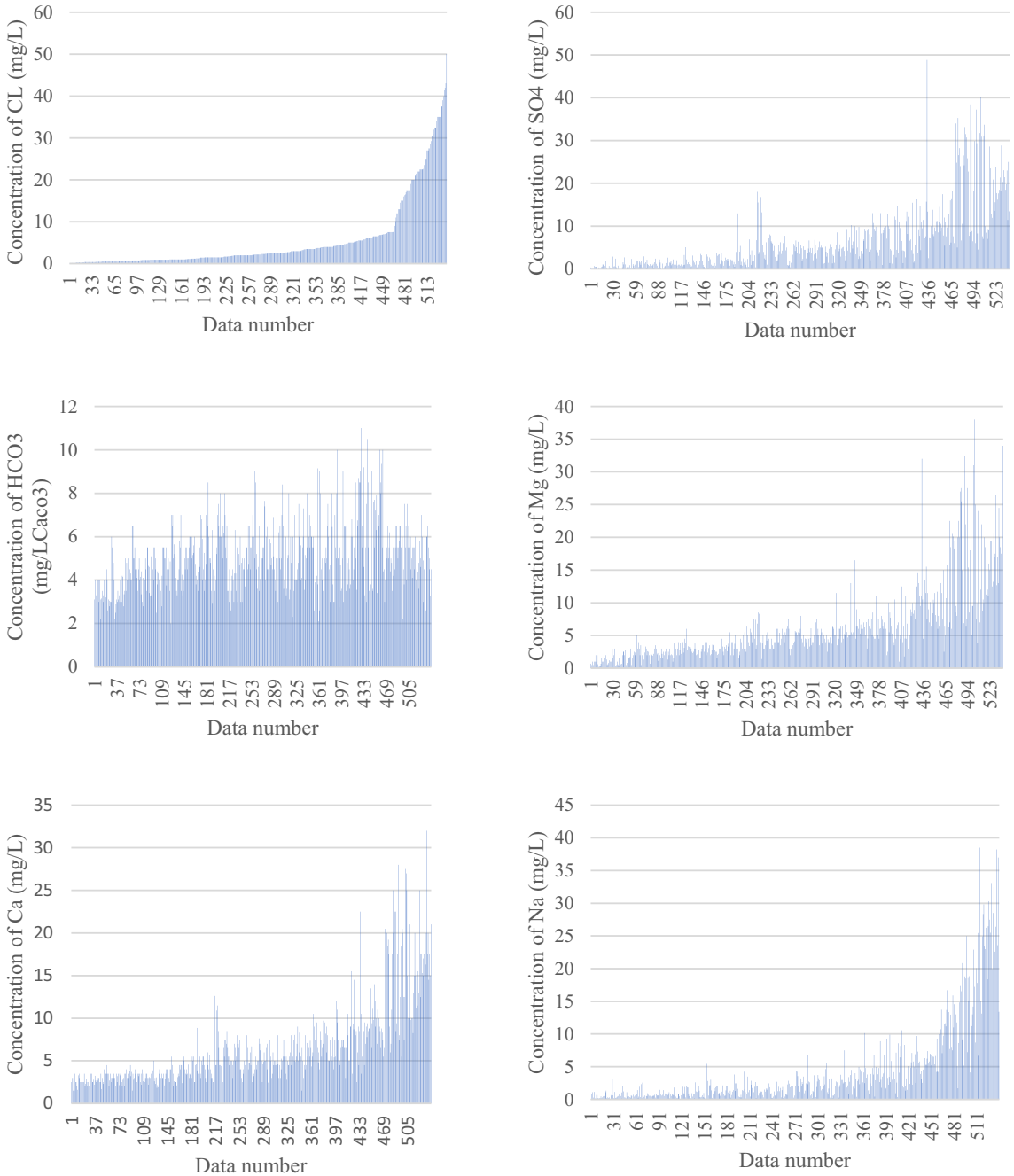

Fig. 1 Diagram showing the variability of values of water quality parameters in groundwater from the study area

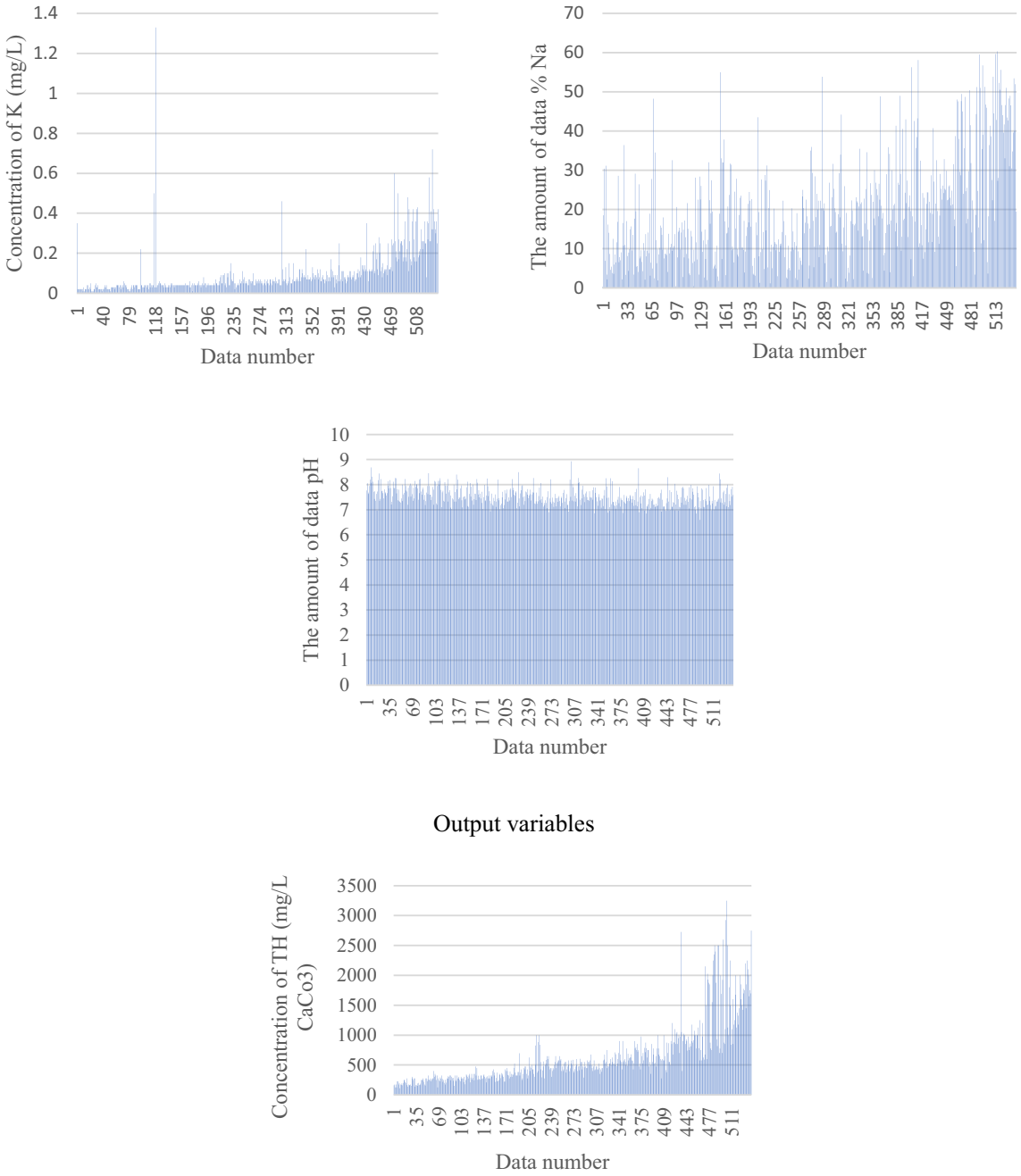

Fig. 1 (continued)

Table 1 Statistical values of measured parameters of groundwater in the study area

Parameters	Input concentration/value (mg/L) for all parameters except (Na% and pH)									Output
	Cl	SO4	HCO3	Mg	Ca	Na	K	Na%	pH	TH (mg/L$CaCo_3$)
Max	50.0	48.9	11.0	38.0	32.1	38.5	1.3	60.3	8.9	3250.0
Min	0.2	0.0	2.0	0.2	1.5	0.0	0.0	0.3	6.6	110.0
Mean	5.5	6.2	5.0	6.2	6.5	4.3	0.1	19.1	7.5	631.8
SD	8.5	7.5	1.6	5.8	5.0	6.5	0.1	13.2	0.4	510.5

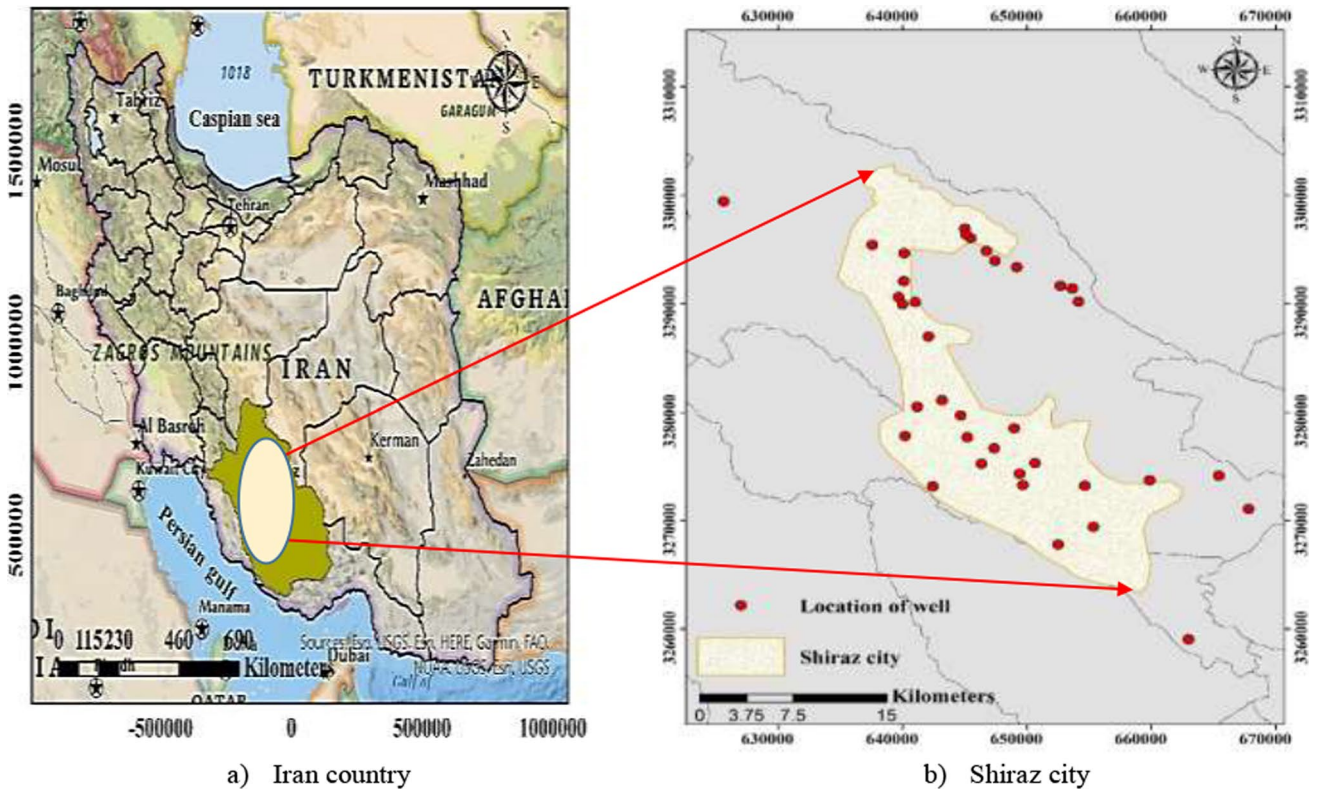

Fig. 2 The location of the study area in the Shiraz Plain

distance weighting method and the ArcGIS Geostatistical Analyst Extension to understand the hardness concentrations in unsampled areas. The sensitivity analysis and evaluation of the relative relevance of each input parameter calculated the percentage influence of geographical and temporal changes on overall hardness. Many algorithms were looked at to choose the one that performed the best with the optimal neural architecture.

In the current study, the novel hybrid models of Teaching Learning-Based Optimization (TLBO), Multiverse Optimizer (MVO), Cuckoo Optimization Algorithm (COA), and Evaporation Rate-based Water Cycle Algorithm (ER-WCA) with Artificial Neural Networks (ANN) were deliberately developed and confirmed by MATLAB coding to predict total hardness (as $CaCO_3$) concentrations for the case study of groundwater in the Shiraz plain in Iran.

Study Area Characterization

In this study, it was necessary to collect data for training purposes, so data were collected from the Shiraz Regional Water Company. This involved the selection of 540 samples from 13 wells in the Shiraz plain that were analyzed in the period from 2002 to 2018. The input parameters for the model were (Cl^-, SO_4^{2-}, HCO_3^-, Na^+, Mg^{2+}, Ca^{2+}, Na percent, K^+, and pH) and the output parameter was (TH). Using the MATLAB R2013 software program, artificial neural network models were developed. Figure 1 and Table 1 show diagrams of inputs and output variables and statistical values of measured parameters of groundwater in the study area.

Description of The Study Area

The Shiraz plain is located in the Iranian province of Fars, and forms part of the watershed for Maharlu lake (Fig. 2). The Shiraz plain spans a region of around 300 km^2 and is situated between longitudes 52,029 and 52,036 and latitudes 29,033 and 29,036. The Shirza plain is surrounded by the Baba Koohi Kaftrak and Drak mountains, which are situated to the north and northwest, respectively. The Shiraz plain is located to the south of Maharlu. The Shiraz plain is underlain by two main aquifers: a shallow aquifer at a depth of about 40 m, and a deeper aquifer at depths of about 40–400 m. The shallow alluvial aquifer is composed of interbedded sand, silt and clay layers of varying thickness. Geophysical measurements of the plain reveal that the quality of groundwater deteriorates with increasing depth (Ahmadi Dehrashid et al. 2024; Ikram et al. 2023;

Badeenezhad et al. 2020; Moayedi et al. 2023b; Rakhshandehroo et al. 2012).

In this study, a comparison is made between a hybrid methodology that incorporates TLBO-ANN, MVO-ANN, COA-ANN, and ER-WCA-ANN with Artificial Neural Networks (ANN) and common ANN, in order to design of the optimal network for assessing groundwater quality. Figure 2 depicts the location of the research region in the Shiraz Plain.

Methodology

Artificial Neural Network

ANNs seek to replicate the operations of the human nervous system within a digital realm, encompassing its architecture (Abiodun et al. 2018; Wang 2003). These networks leverage artificial neural connections to predict or approximate a function. In a standard artificial neural network (ANN), there are concealed layers between the input and output structures for feature adjustments. The ANN model illustrated in this document is shown in Fig. 3.

Over the past few decades, there has been a significant increase in the utilization of neural networks for prediction and classification tasks. These networks typically consist of an input layer, an output layer, and at least one hidden layer. The input data provided to these networks is usually split into two distinct sets for training, learning, and testing purposes. An ANNs comprises multiple perceptrons or neurons at each layer, and when the input data flows in a forward direction, this architecture is referred to as a feed-forward neural network. An ANN typically consists of three primary layers: input, hidden, and output. Data is received by the input layer, processed by the hidden layers, and then returned by the output layer (Feindt and Kerzel 2006; Salari et al. 2018). These neural network layers are responsible for learning the optimal weights that are applied at the conclusion of the training process.

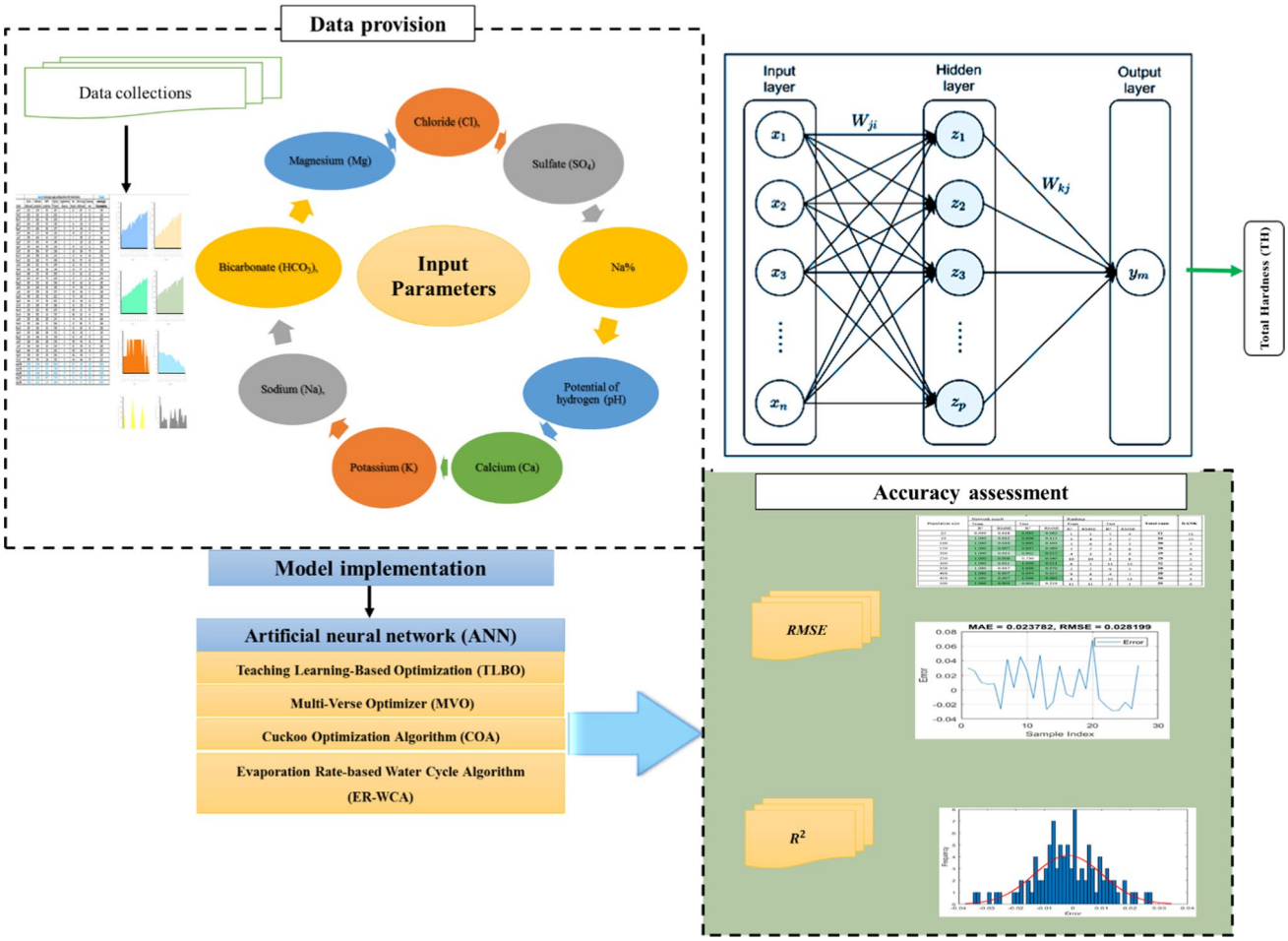

Fig. 3 The basic structure of the ANN-MLP that was developed in the current study

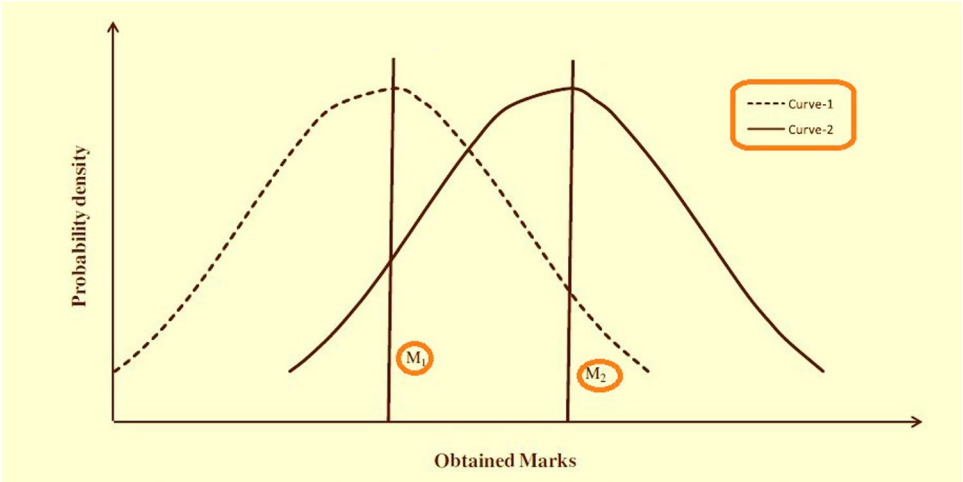

Fig. 4 Distribution of grades of students who took classes from two teachers after (Rao et al. 2011)

ANNs are proficient in handling various data types such as text, images, and tabular data. One key advantage of ANNs is their ability to effectively transform any input into an output, especially when dealing with nonlinear functions and learning optimal weights. The nonlinear activation functions within ANNs enable them to achieve a universal approximation, meaning they can learn complex relationships between input and output data. As a result, an increasing number of scientists are turning to ANNs for their research (Prakash et al. 2021). The proposed technique utilizing ANNs was implemented and evaluated on a custom-built integrated forecasting program developed in MathWorks MATLAB.

Teaching–Learning-Based Optimization (TLBO)

Consider two distinct classes of students with the same merit level who are being instructed in the same subject by two separate teachers, T_2 and T_1. Figure 4 depicts the distribution of grades earned by students in two distinct courses, as determined by the professors. The grades of the students instructed by instructors T_2 and T_1 are represented by curves 2 and 1, respectively. It is believed that the obtained markings have a regular distribution, but it is possible that this is not the case. The normal distribution is defined by the following:

$$f(x) = \frac{1}{\sigma\sqrt{2\pi}} e^{\frac{-(x-\mu)^2}{2\sigma^2}} \quad (1)$$

in which μ stands for the mean, σ^2 is the variance, and any value for which a normal distribution function is required is represented by the symbol x (Rao et al. 2011).

Curve-2 outperforms curve-1 in terms of results, as shown in Fig. 4. Thus, it might be claimed that the teacher T_1 performs weaker than the teacher T_2 in terms of teaching. The mean of the two outcomes (M_1 for the curve-1 and M_2 for curve-2) is the main distinction. This implies that more significant learning outcomes are the product of better teachers. Students also gain knowledge from their interactions with one another. This fact also aids them in achieving more remarkable outcomes (Hudcovic 2022).

Figure 4 shows a model for the grades of students in a class with a curve "A" (e.g., here we have curve one or curve 2) and a mean of "M_A" (e.g., here we have M_1 and M_2) attained. A community's most knowledgeable member is thought of as a teacher. The best learner can, therefore, be imitated as a teacher, as T_A in Fig. 4 demonstrates. The teacher wants to help students succeed academically and spread knowledge throughout the class to raise everyone's level of understanding. As a result, a teacher might raise the class average based on their abilities. Figure 4 demonstrates how a teacher "T_A" will make an effort to raise learners' levels to a newer mean M_B by moving the mean M_A nearer their level, following their capabilities. Nevertheless, the teacher T_A will give teaching their students their full attention. The quality of the teacher's instruction and the number of pupils in the class will determine how much knowledge the students will gain. The mean value throughout the community may be used as a metric to assess the caliber of the students. Teacher T_A will make an effort to raise the caliber of the students from M_A to M_B. They require a new teacher of a higher caliber than they are. This indicates that T_B is the new instructor in this instance. As a result, a new curve B will be there, and the teacher T_B.

Teaching–Learning-Based Optimization is based on a population strategy that uses a population of solutions to advance toward the overall solution, like the other algorithms inspired by nature (Almutairi et al. 2022). The population of a Teaching–Learning-Based Optimization is a class or group of students. Different design variables are included

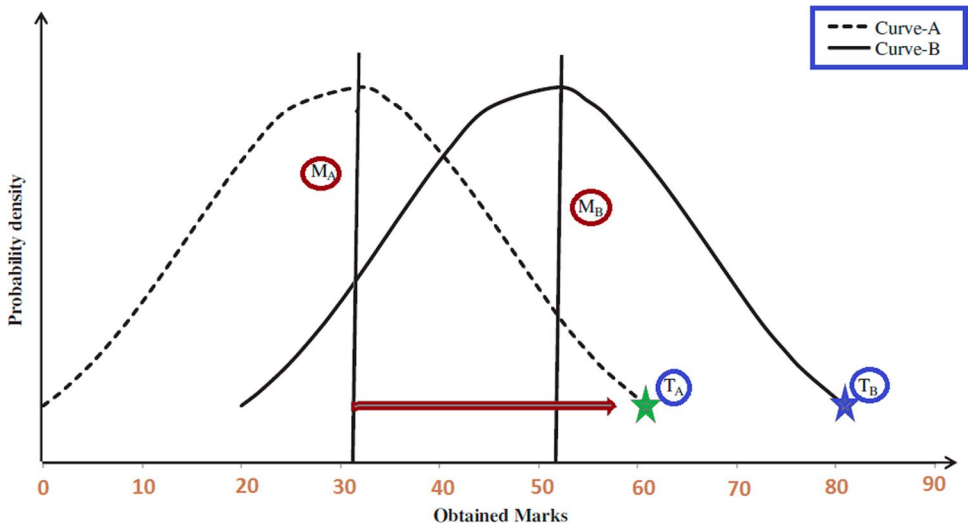

Fig. 5 Model for the acquired mark distribution of a group of students

in the population using optimization methods. The learners' results will be analogous to the 'fitness' in Teaching–Learning-Based optimization, and various design variables will be comparable to different subjects offered to learners, much like others based on population optimization systems. The teacher is thought to be the best discovery so far. The Teaching–Learning-Based optimization process may be divided into two sections, the first of which contains the "teacher phase" and the second of which includes the "learner phase." The "Learner Phase" is considered mutual learning through learner interactions, whereas the "Teacher Phase" is understood as receiving instruction from the teacher (Rao et al. 2011).

Teacher phase

Figure 5 illustrates how having an excellent instructor can enhance a class's meaning from M_A to M_B. Good teachers help their students advance their level of knowledge. Nonetheless, this is almost impossible, and a teacher can somewhat raise a class's mean in terms of its capacity. Concerning several variables, this follows a random process.

Assume that M_i is cruel and T_i stands in for the instructor at any given iteration. The new mean, designated as M_{new}, will be the same as T_i entitled, as it will strive to raise the mean M_i to its level. The difference between the new and old means presented will be used to update the solution.

$$Difference\_mean_i = r_i(M_{new} - T_F M_i) \tag{2}$$

where r_i is a random digit between [0, 1] and T_F denotes a teaching term that causes the mean point to be shifted. Since as T_F= round[1 + rand(0,1)(2 _ 1)], the value of T_F is assumed to be 1 or 2, likewise a probationary stage selected randomly by equal chance.

A difference of this kind modifies the existing solution to satisfy the following expression.

$$X_{new,i} = X_{old,i} + Difference\_mean_i \tag{3}$$

Learner phase

There are two ways for learners to increase their knowledge: through interactions with one another and, secondly, through teacher input. Through formal communications, presentations, group debates, etc., a learner interacts randomly with other learners and picks up new information if the other learners are more experienced than they are. The learner modification might be defined as

For $i = 1$; P_n
Randomly select another learner X_j, such that $i \neq j$.
If $f(X_i) < f(X_j)$
$X_{new,i} = X_{old,i} + r_i(X_i - X_j)$
Else
$X_{new,i} = X_{old,i} + r_i(X_j - X_i)$
End If
End For
Accept X_{new} if it gives a better function value.
Figure 6 contains the flowchart of the TLBO technique.

Multi-Verse Optimizer

The multiverse optimizer (MVO) method was expanded by Mirjalili et al. (2016) based on the multiverse physics theory. According to the multiverse hypothesis, there have been

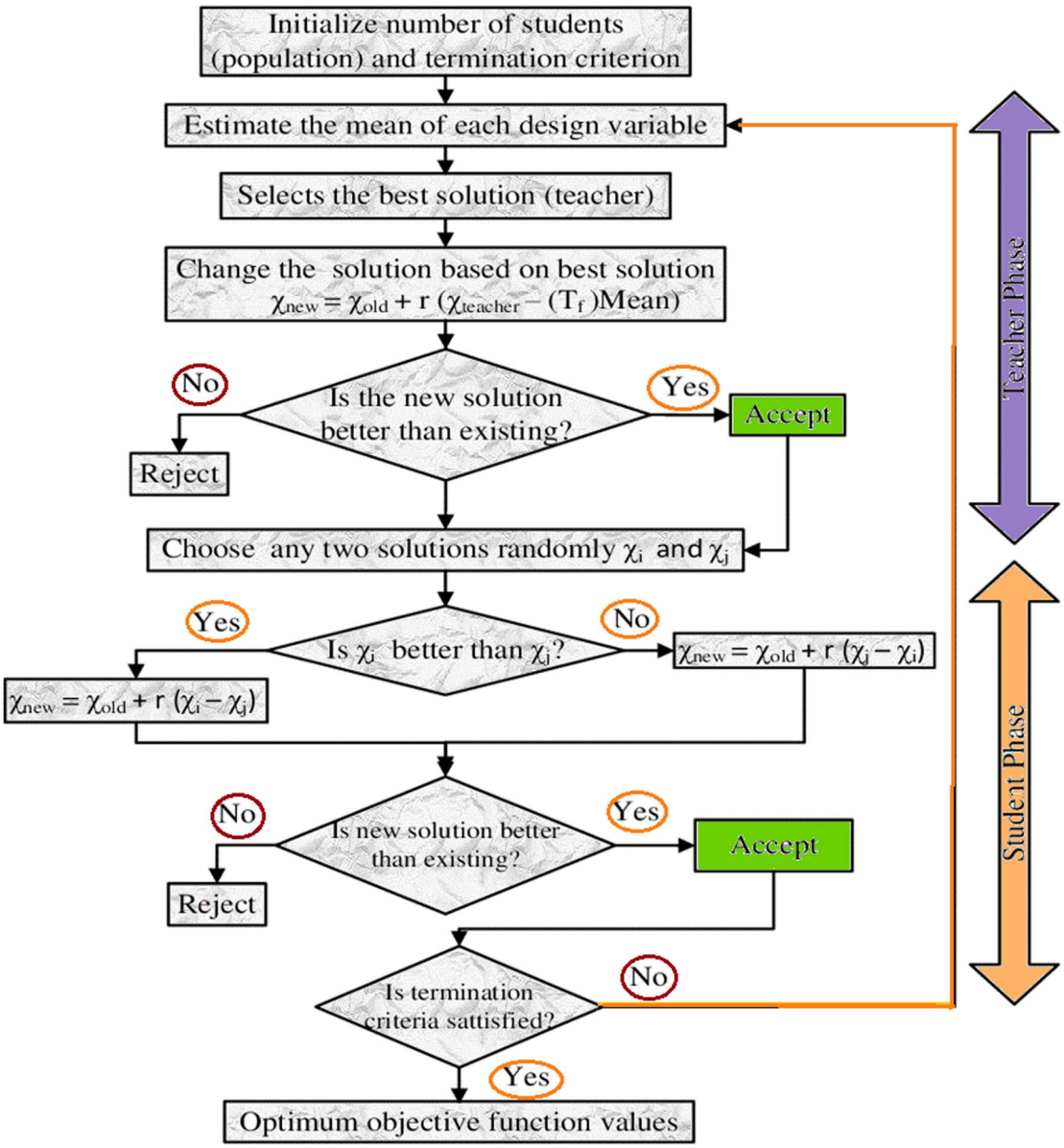

Fig. 6 Diagram showing the TLBO algorithm's process after (Rao et al. 2011)

multiple big bangs, each of which created a universe (Mirjalili et al. 2016; Moayedi and Mosavi 2021). It makes a mathematical model of the wheel mechanism that transports universe goods and the wormhole (white/black) tunnels that link the two worlds. After each iteration, (1) the inflation rates of the universes are ranked, and then (2) a roulette wheel selects the universe with the highest inflation rate to contain a white hole. The MVO model is described below in mathematical terms.

Consider the following:

$$u = \begin{bmatrix} x_1^1 & x_1^2 & \cdots & x_1^d \\ x_2^1 & x_2^2 & \cdots & x_2^d \\ \vdots & \vdots & \vdots & \vdots \\ x_n^1 & x_n^1 & \cdots & x_n^d \end{bmatrix} \tag{4}$$

If n is the total number of universes (possible solutions) and d is the total number of parameters (variables), then (Mirjalili et al. 2016):

$$x_k^j = \begin{cases} x_k^j r_1 < NI(u_i) \\ x_i^j r_1 \geq NI(u_i) \end{cases} \quad (5)$$

where r_1 is an integer between 0 and 1, u_i is the i-th universe, $NI(u_i)$ is the i-th universe's normalized inflation rate, and x_i^j is the i-th world's j-th parameter (Mirjalili et al. 2016; Moayedi and Mosavi 2021).

Assuming a wormhole conduit connects one planet to the greatest universe, the method of transportation is as follows (Mirjalili et al. 2016):

$$x_i^j = \begin{cases} \begin{cases} x_j + TDR + \left(\left(ub_j - lb_j\right) * r_4 + lb_j\right) if r_3 < 0.5 \\ x_j - TDR + \left(\left(ub_j - lb_j\right) * r_4 + lb_j\right) if r_3 \geq 0.5 \end{cases} & r_2 < WEP \\ x_i^j r_2 \geq WEP \end{cases} \quad (6)$$

where lb_j and ub_j are the lower and upper values of the j-th variable, x_j is the j-th parameter of the best universe, WEP and TDR are the worm existence probability and traveling distance rate, respectively, and r_2, r_3, and r_4 are random values between [0, 1]. The WEP and TDR formulas are as follows:

$$WEP = MIN + l \times \left(\frac{max - min}{L}\right) \quad (7)$$

$$TDR = 1 - \frac{l^{1/p}}{L^{1/p}} \quad (8)$$

L is the total number of iterations conceivable, where l is the current iteration, p represents the exploitation accuracy over iterations, which is set to 6, and minimum and maximum values are represented by min and max, which are set to 0.2 and 1, respectively (Moayedi and Mosavi 2021). Using 30 universes, the number of iterations allowed in this investigation is 500.

Cuckoo Optimization Algorithm (COA)

The Cuckoo Optimization Algorithm (COA), a technique for optimization, takes its cues from the behavior of cuckoo birds. Yang and Deb presented the COA for the first time (Yang and Deb 2009), but this was elaborated by Rajabioun (2011). This method is one of the best optimization techniques, and it has a remarkable ability to find global optimums. The COA starts with a basic population, in this example a population of cuckoos, just as other evolutionary algorithms. These cuckoos are known as hosts because they lay their eggs in the nests of other bird species. The host will recognize and kill any cuckoo eggs that closely resemble its own eggs, which have a higher chance of surviving and growing into adult cuckoos. The number of eggs that hatch indicates how suitable a habitat is for the host nests. A given setting will be more valued the more eggs that hatch there. Therefore, the spot where the most eggs may survive is the concept that the COA aims to improve. To put it another way, cuckoos look for the best location to collect their eggs in order to maximize the probability that their offspring will survive.

The cuckoo eggs that survive hatch into adults, creating a new cuckoo population. This population migrates farther toward the best (or most advantageous) environment available but cannot stray too far from where they are now. An egg-laying radius determines the appropriate migratory range. The egg-laying radius is influenced by a cuckoo's total number of eggs and distance from the ideal environment. As a result, more cuckoos begin randomly laying eggs throughout the projected egg-laying radius. The best egg-laying site (i.e., the habitat with the maximum benefit) is not found until this cycle has repeated itself several times. This is where the vast bulk of cuckoos congregate.

When the problem parameters are arranged into a habitat matrix, the COA should be employed to resolve the optimization problem. An N_{var}-The dimensional optimization problem's habitat is a collection of the following $1 \times N_{var}$ cuckoo placements (Akbarzadeh and Shadkam 2015).

$$\text{Habitat} = \left[X_1, X_2, \ldots, X_{Nvar}\right] \quad (9)$$

The profit of the habitat is determined by evaluating the profit function. f_p for the current habitat:

$$\text{Profit} = f_p(\text{Habitat}) = f_p(X_1, X_2, \ldots, X_{Nvar}) \quad (10)$$

An algorithm for optimizing profits is the COA (Akbarzadeh and Shadkam 2015). Consequently, minimization problems are evaluated using the continuing function :

$$\text{Profit} = -\text{Cost}(\text{Habitat}) = -f_c(X_1, X_2, \ldots, X_{Nvar}) \quad (11)$$

A method for population optimization begins by creating a habitat matrix of size $N_{opt} \times N_{var}$ and they assign a random number of eggs to each habitat. A cuckoo can produce between 5 and 20 eggs in the wild. As a result, these numbers are frequently used to determine the minimum and maximum egg-laying rates per cuckoo per repetition. The egg-laying radius (ELR), or maximum radius from the cuckoo's current location, is where cuckoos lay their eggs (Adnan Ikram et al. 2023; Moayedi et al. 2024). All parameters in an optimization problem have upper and lower bounds, denoted by the variables. Var_{hi} and Var_{low}, respectively:

$$ELR = \alpha \frac{\text{Number of cuckooo}'\text{s eggs}}{\text{Total number of eggs}} \times (\text{Var}_{\text{hi}} - \text{Var}_{\text{low}}) \quad (12)$$

where a is the parameter that modifies the ELR maximum value, within its ELR, each cuckoo has a host nest where

eggs are randomly laid. Once all the cuckoos have successfully set their eggs, the host bird searches for and eats any cuckoo eggs that are least like its own. Mathematically, a fixed percentage (usually 10%) of the cuckoo eggs with the lowest profit function value are rejected, while the other eggs hatch and start a new colony (Akbarzadeh and Shadkam 2015; Rajabioun 2011).

Evaporation rate-based water cycle algorithm

Sadollah and colleagues (2015) suggested the ER-WCA through adjustments made to the water cycle algorithm. This optimizer, based on population, has demonstrated proficiency in addressing different regression concerns (Foong et al., 2021)and classification issues (Alweshah et al., 2020). The foundational concept behind this approach lies in the WCA algorithm (Eskandar et al., 2013), which emulates the natural water cycle described by David (1993). The algorithm replicates processes such as water transpiration, evaporation leading to cloud formation, and subsequent precipitation returning the water back to the earth in various forms.

In terms of convergence speed and precision, the WCA surpasses many other optimizers (Eskandar et al., 2013). The algorithm's performance across all dimensions contributes to this comparative advantage (Sadollah et al., 2016). When compared to the binary version of WCA, the ER-WCA strikes a better balance between exploitation and exploration, leading to enhanced precision and quicker convergence (Sadollah et al., 2015). The algorithm can be broken down into several stages. Initially, the population is randomly generated, forming initial entities (referred to as streams, rivers, and seas). Each stream is subjected to a cost function to oversee error minimization. Subsequently, the flow intensity (FI) for these entities is computed, and their positions are adjusted accordingly. Rivers flow towards the sea, with the evaporation rate (ER) being determined. Member positions are updated based on the acquired ER. Below are some mathematical explanations. By regarding well-fitted entities as rivers and others as streams, the candidate streams (CS) array can be defined as shown (Hussien et al., 2022):

$$CS = \left[x_1, x_2, \ldots, x_K\right] \tag{13}$$

in which K represents the dimension of the problem. Assuming K_{pop} as the population size, generating the population is expressed by Eq. (2):

$$Total\ population = \begin{bmatrix} Sea \\ River_1 \\ River_2 \\ \vdots \\ Stream_{K_{sr+1}} \\ Stream_{K_{sr+2}} \\ \vdots \\ Stream_{K_{pop}} \end{bmatrix} = \begin{bmatrix} x_1^1 & x_2^1 & \cdots & x_K^1 \\ x_1^2 & x_2^2 & \cdots & x_2^K \\ \vdots & \vdots & \ddots & \vdots \\ x_1^{K_{pop}} & x_2^{K_{pop}} & \cdots & x_N^{k_{pop}} \end{bmatrix} \tag{14}$$

Equation (3) gives the FI:

$$Cost_i = f\left(x_1^i, x_1^i, \ldots, x_K^i\right) i = 1, 2, \ldots, K_{pop} \tag{15}$$

Moreover, Eqs. (4) and (5) reflect the process of designating the streams to the rivers and the sea:

$$C_n = Cost_n - Cost_{K_{sr+1}} n = 1, 2, \ldots, K_{sr} \tag{16}$$

$$NS_n = round\left\{\left|\frac{C_n}{\sum_{n=1}^{K_{sr}} C_n}\right| \times K_{streams}\right\}, n = 1, 2, \ldots, K_{sr} \tag{17}$$

where K_{sr} shows the number of individuals who opted for the best-fitted ones. Subsequently, K_{Stream} denotes the number of the remaining individuals (Hussien et al. 2022).

Results

The precision of the statistical parameters of ANN models was reported. Coulibaly et al. (1999) demonstrated that for most prediction problems, a single hidden layer may suffice to generate multiple trial results. Consequently, the MLP model (ANN) utilized in this investigation contained only one hidden layer. After each training session, the test data set was used to calculate RMSE, R^2, and MAE to determine the optimal number of hidden nodes for the input layer. The multilayered preceptor utilized between one and fifty concealed nodes (Khashei-Siuki et al. 2011).

The data sets used to assess the portion of the neural network were compared to observed values and a determined ANN. The determination coefficient (R^2), root mean square error (RMSE), and mean average errors (MAE) were the statistical indices used in this comparison:

$$R^2 = \left[\sum_{i=1}^{N}(P_i - \overline{P})(O_i - \overline{O})\right]^2 \left[\sum_{i=1}^{N}(P_i - \overline{P})(O_i - \overline{O})\right]^{-1} \tag{18}$$

$$RMSE = \left[N^{-1} \sum_{i=1}^{N} \left(P_i - O_i \right)^2 \right]^{0.5} \quad (19)$$

$$MAE = \frac{1}{N} \sum_{i=1}^{N} \left(P_i - O_i \right) \quad (20)$$

P and O represent the mean values for P_i and O_i, where N is the number of observations, P_i represents the estimated values (as determined by the ANN and ANFIS), O_i represents the observed data and P_i represents the estimated data. The data set for testing ANNs was also used to compare the chosen ANN with the conventional method, contributing to an exceptional outcome. In this comparison, three statistical criteria were utilized, and the finest degree was determined after the degrees were sorted into classes.

The objective of this paper was to model TH values using two distinct soft computing techniques and two modeling scenarios. In the following sections, the summary statistical analysis of the model's performance accuracy for both adopted scenarios will be presented (Figs. 7, 8, 9, 10, 11, 12, 13, 14).

This section summarizes the RMSE and MAE values calculated for the TLBO, MVO, COA, and ER-WCA output variables. This diagram illustrates the precision obtained when using ideal values for each index. Note that RMSE and R^2 should be zero and one, respectively. This finding also holds true for the remaining indices' precision

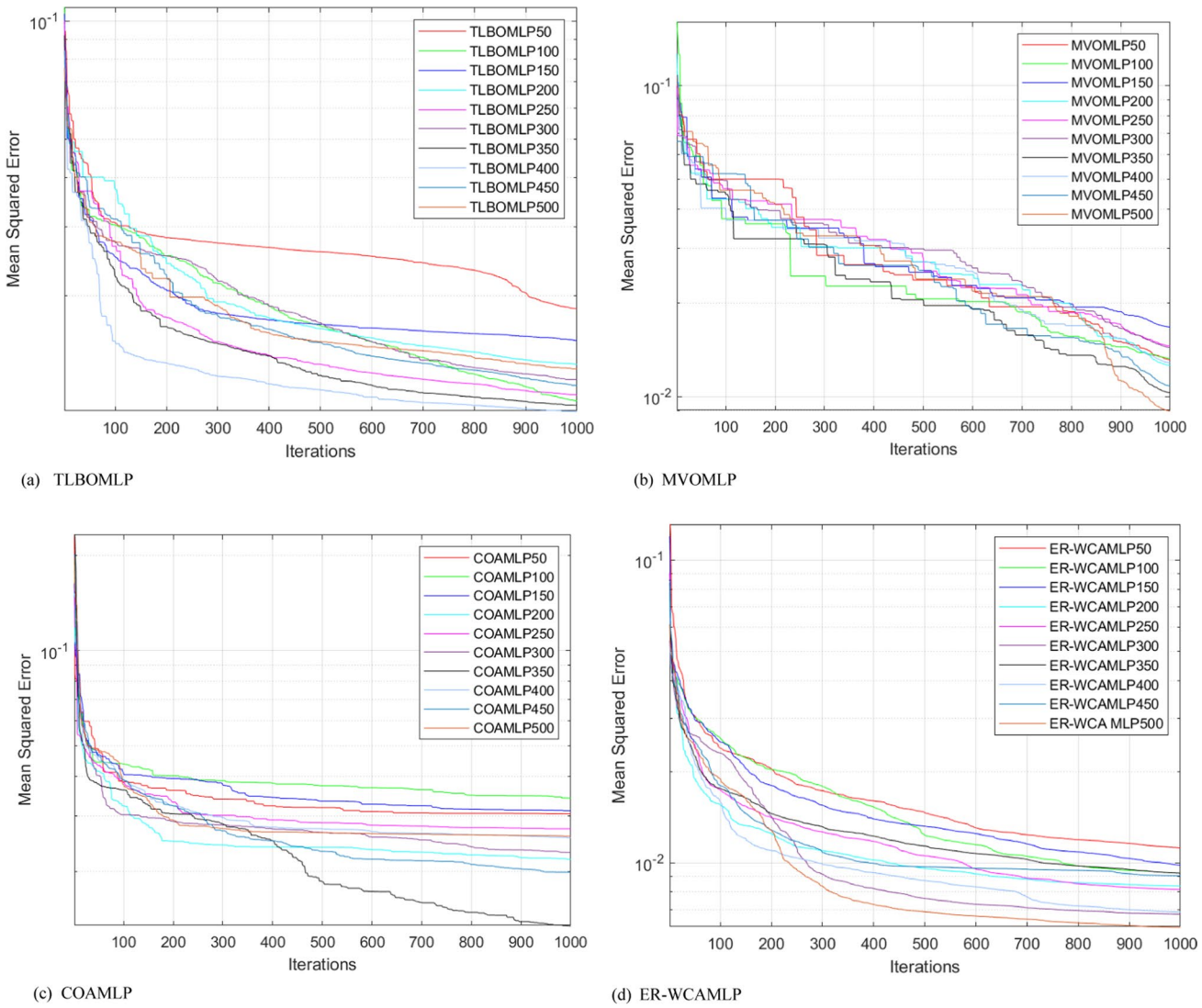

Fig. 7 The best fit model for the TLBOMLP, MVOMLP, COAMLP, and ER-WCAMLP assessments

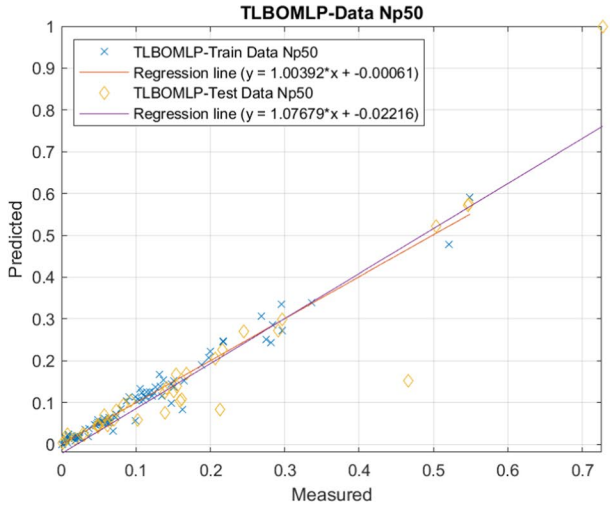

(a) TLBOMLP- N_p50

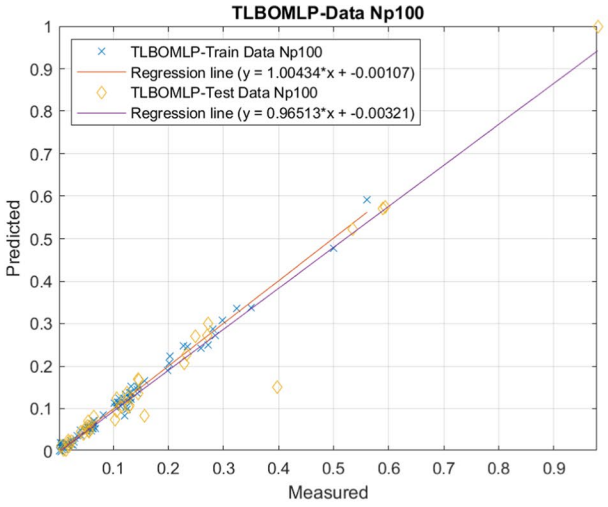

(b) TLBOMLP - N_p100

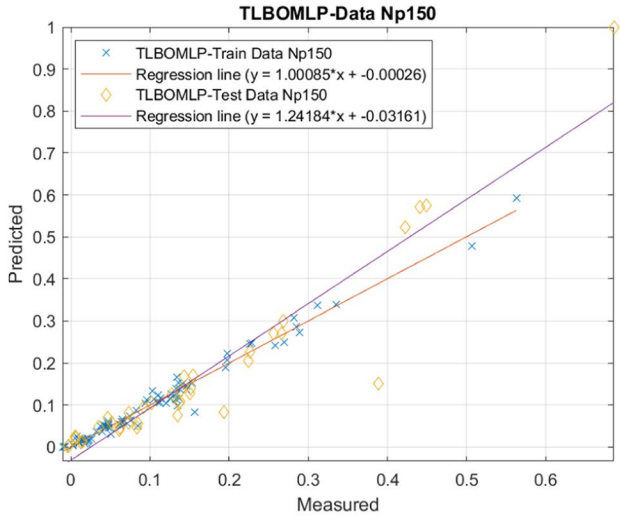

(c) TLBOMLP - N_p150

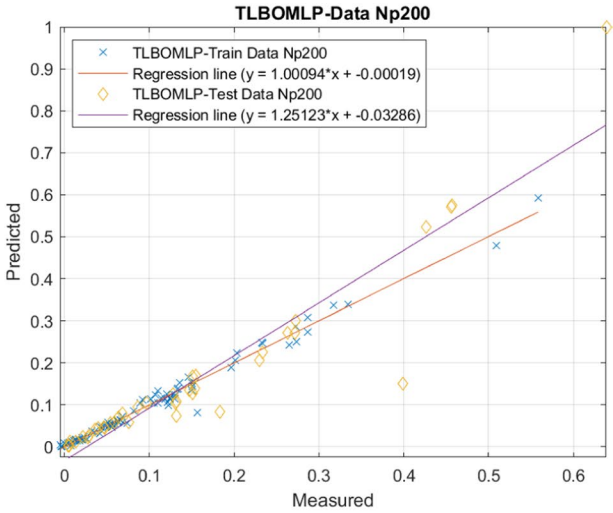

(d) TLBOMLP - N_p 200

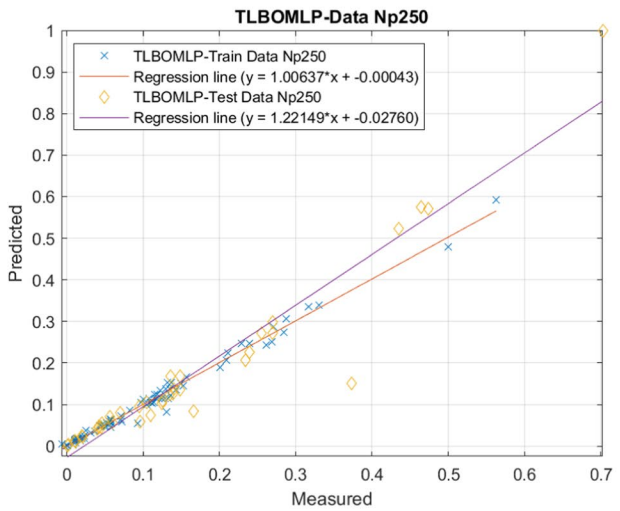

(e) TLBOMLP - N_p250

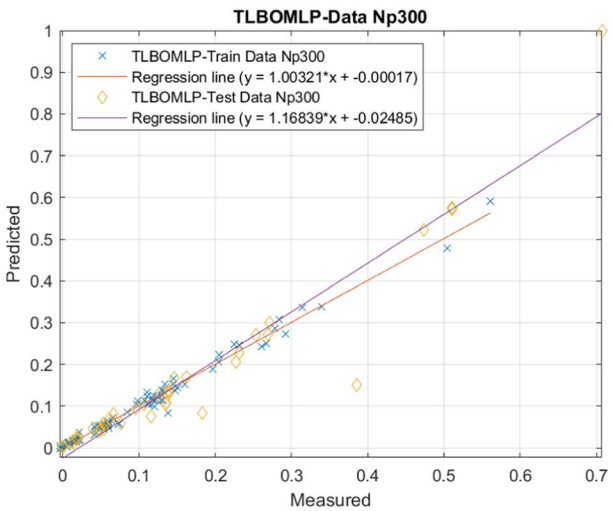

(f) TLBOMLP - N_p300

Fig. 8 Training and testing dataset accuracy results for several suggested TLBOMLP structures

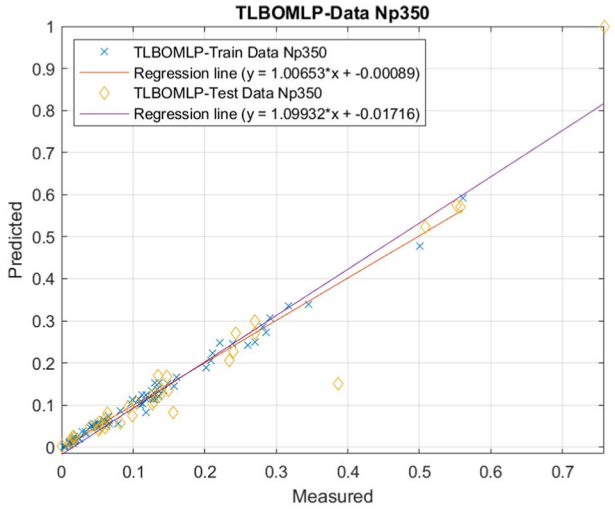

(g) TLBOMLP - N_p350

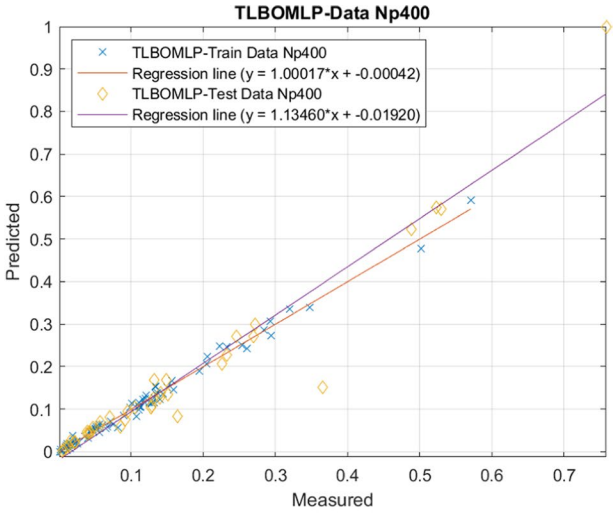

(h) TLBOMLP - N_p400

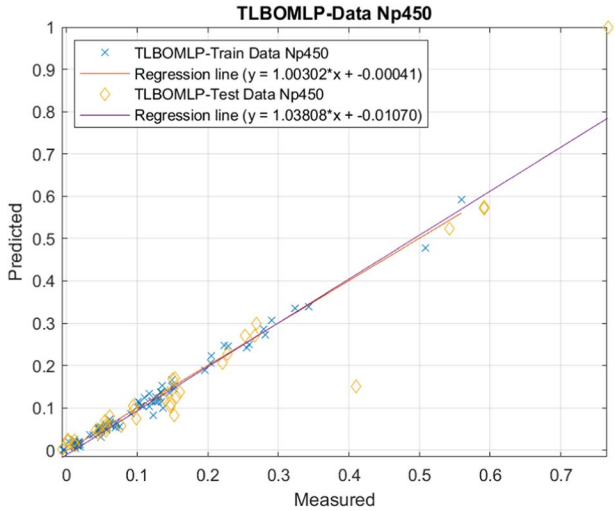

(i) TLBOMLP - N_p450

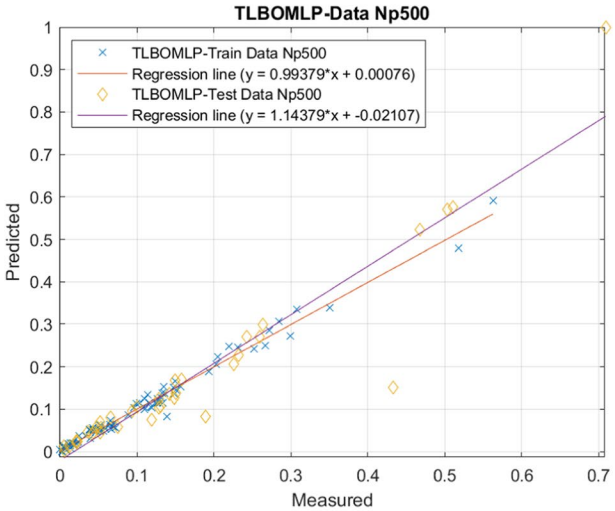

(j) TLBOMLP - N_p500

Fig. 8 (continued)

and accuracy. Please note that before performance indices can be generated, the percentage numbers must be converted to decimals. Figure 15 shows the MSE value for TLBO, MVO, COA, and ER-WCA for ten population sizes (50, 100, 150, 200, 250, 300, 350, 400, 450, and 500) in the current research as a function of iterations (1000 iterations).

As for the model ranking, the model with the highest value was given the highest rank (corresponding to the number of models under consideration), and the model with the lowest value was given the lowest rank (1 for training and assessment results). The total score was then calculated by adding their respective essential obtained score (from each training and testing calculation phase). With a population size of 500 (e.g., R^2 values equal to 0.9983 and 0.98261, and RMSE values equal to 0.03698 and 0.00611 in the training and testing datasets, respectively), the ER-WCAMLP approach proposed the most accurate prediction network for calculation the TH. On the COAMLP, the population of 350 has the worst R^2 (0.9919 and 0.94239) and the worst RMSE (0.01336 and 0.03698), making it the least reliable model for forecasting TH. It is necessary to compare the outcomes of this research with those from other studies to assess the suggested technique's efficacy. Consideration should be taken while comparing similar datasets.

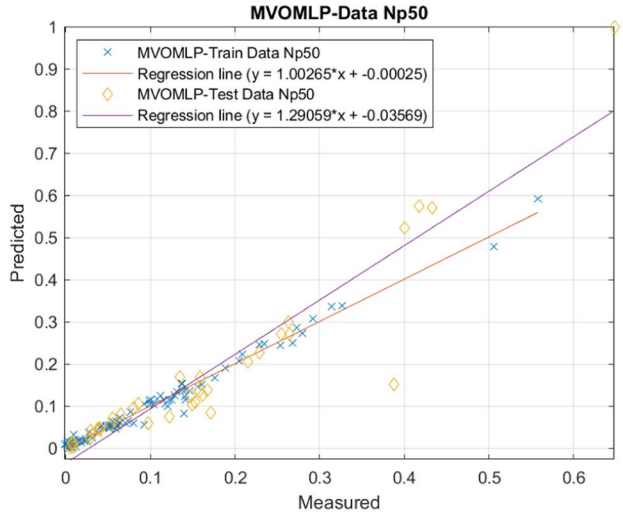

(a) MVOMLP- N_p50

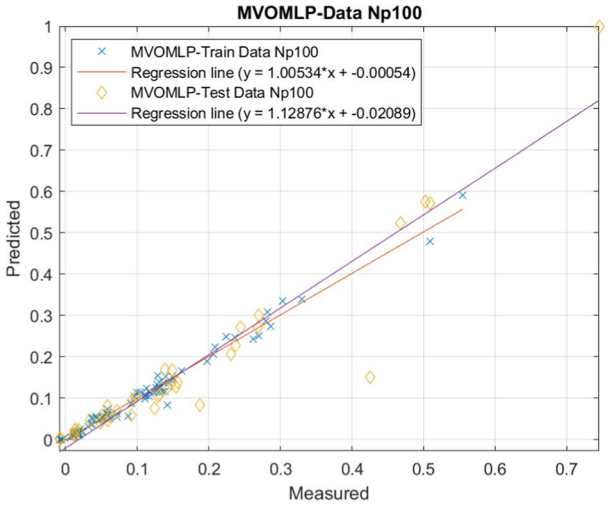

(b) MVOMLP - N_p100

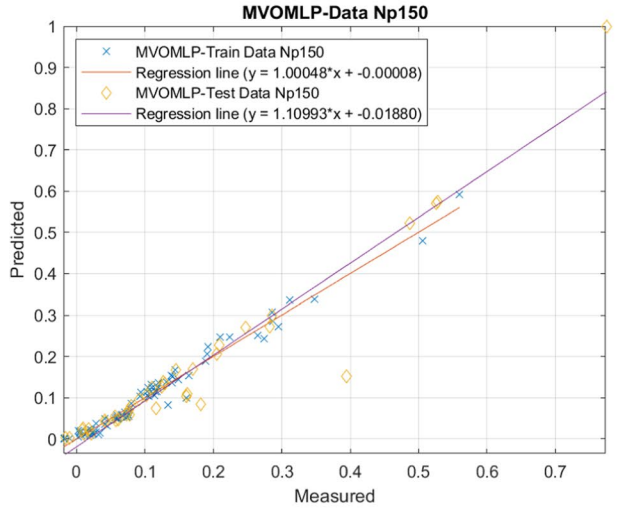

(c) MVOMLP - N_p150

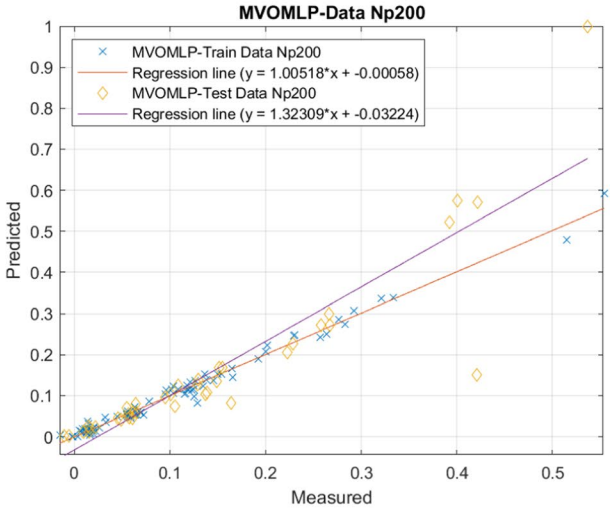

(d) MVOMLP - N_p 200

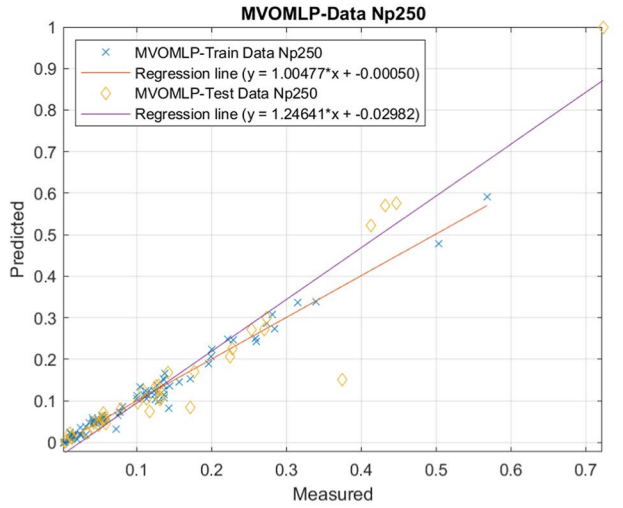

(e) MVOMLP - N_p250

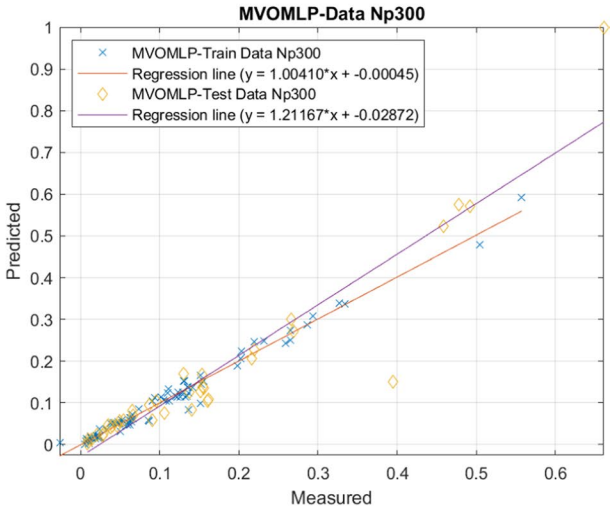

(f) MVOMLP - N_p300

Fig. 9 Training and testing findings from many datasets recommended MVOMLP structures

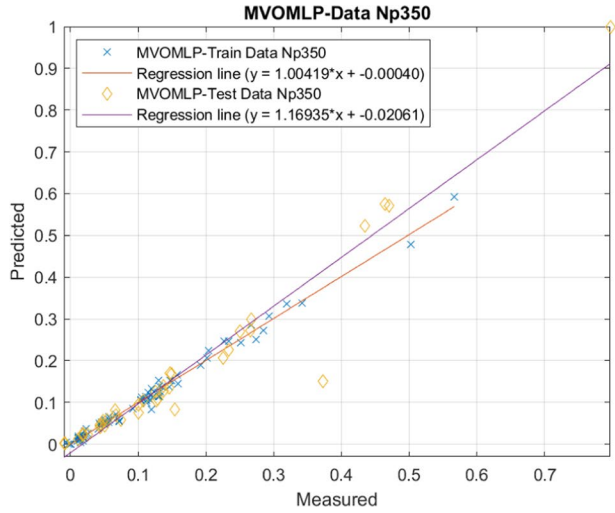

(g) MVOMLP - N_p350

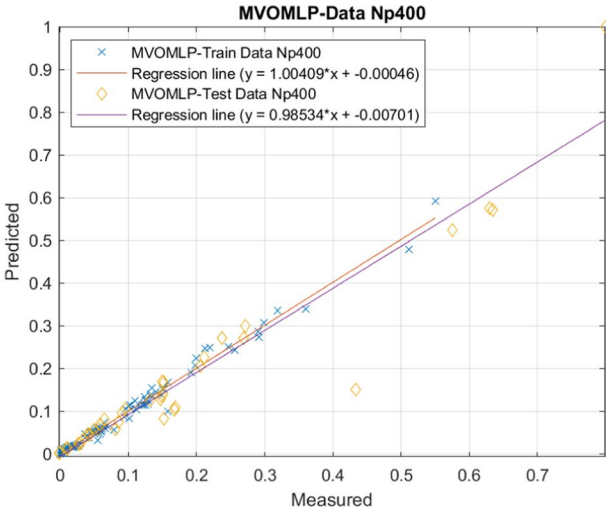

(h) MVOMLP - N_p400

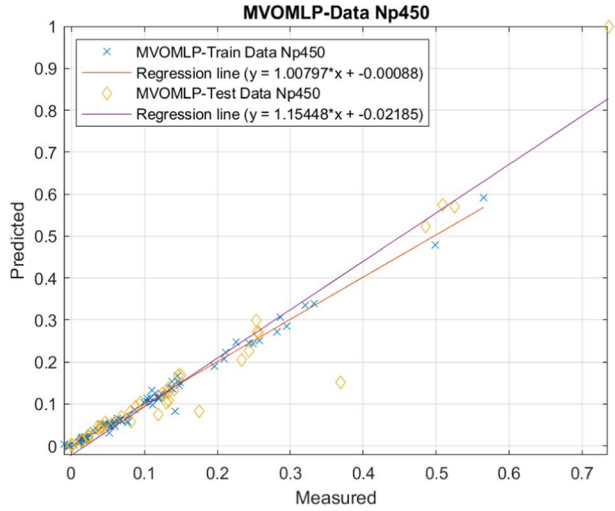

(i) MVOMLP - N_p450

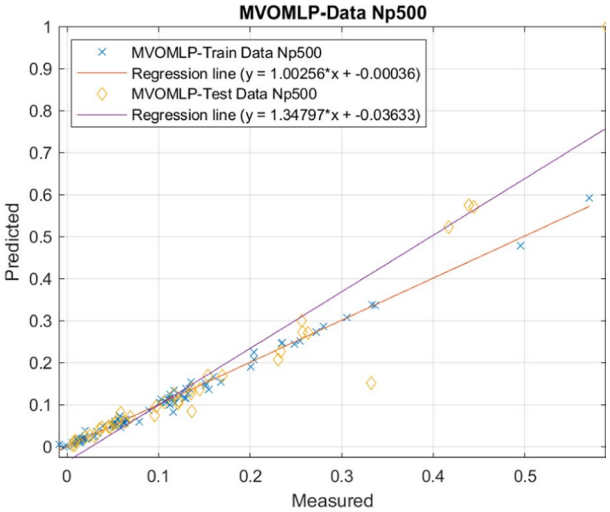

(j) MVOMLP - N_p500

Fig. 9 (continued)

The recommended hybrid models' regression outlines are shown in Tables (6–9). The R^2 measures the correlation potential, with a value of one denoting the best-case scenario and zero representing the worst-case scenario, as previously mentioned. The correlation between predicted and actual values that is as little as possible is 0 or 1. For population sizes of 400, 350, 350, and 500, respectively, the best prediction models (based on the TLBO, MVO, COA, and ER-WCA models) were found after 40,000 modeling iterations using the predefined accuracy indices.

Discussion

Tables 2, 3, 4, 5 and 6 showed network outcomes for different suggested TLBOMLP, MVOMLP, COAMLP, and ER-WCAMLP swarm sizes based on two statistical indices (R^2, RMSE). It is feasible to determine that the advised course of action has been sufficiently evaluated with the objective data by examining and assessing the following figures, which show the first testing and training stages of the ER-WCAMLP network for ten population sizes. The results show that the network was correctly trained, and the architecture for most

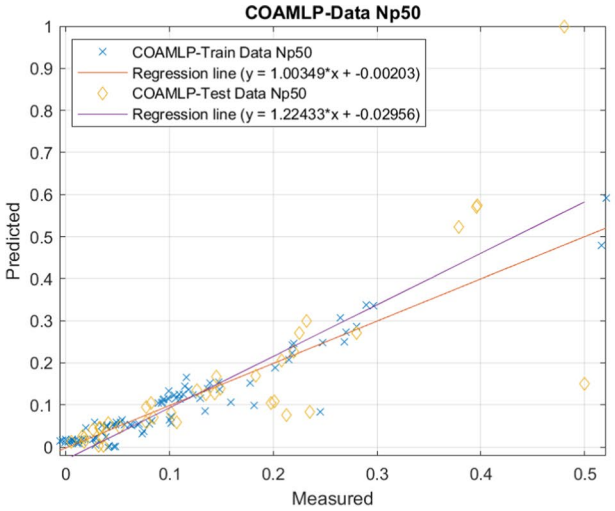

(a) COAMLP- N_p50

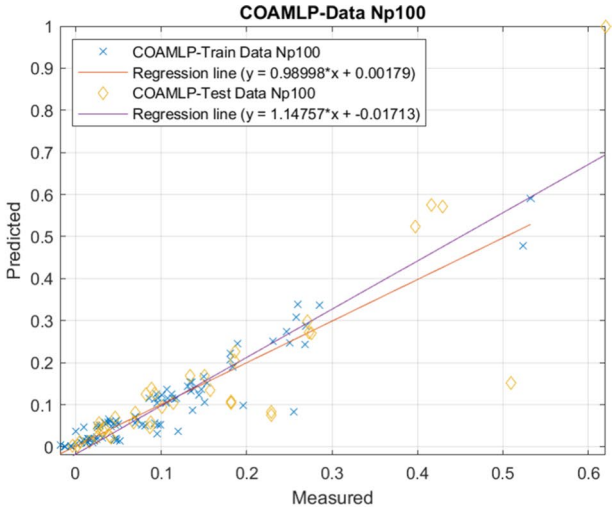

(b) COAMLP - N_p100

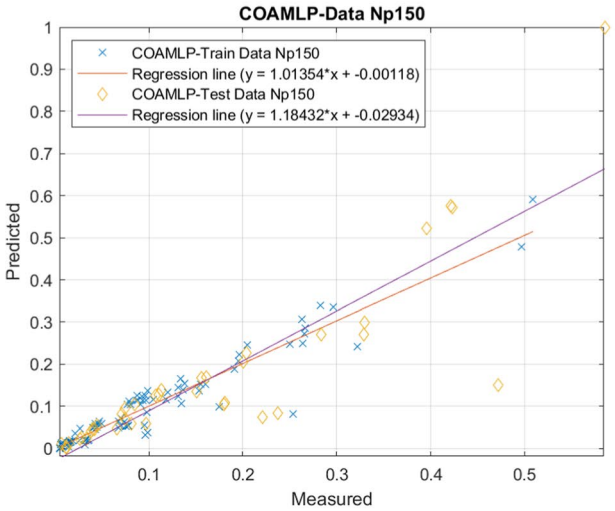

(c) COAMLP - N_p150

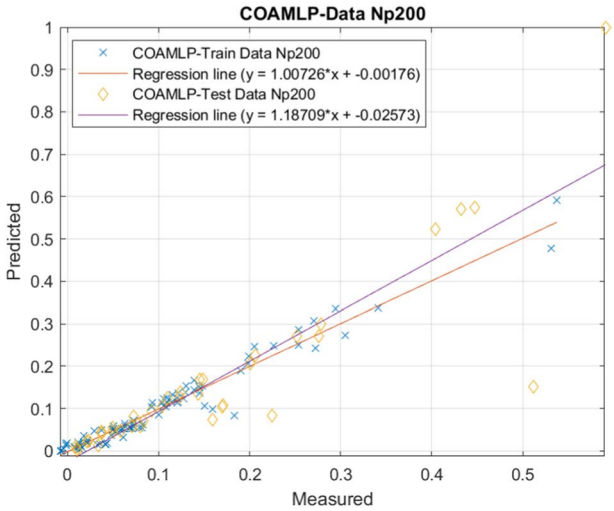

(d) COAMLP - N_p 200

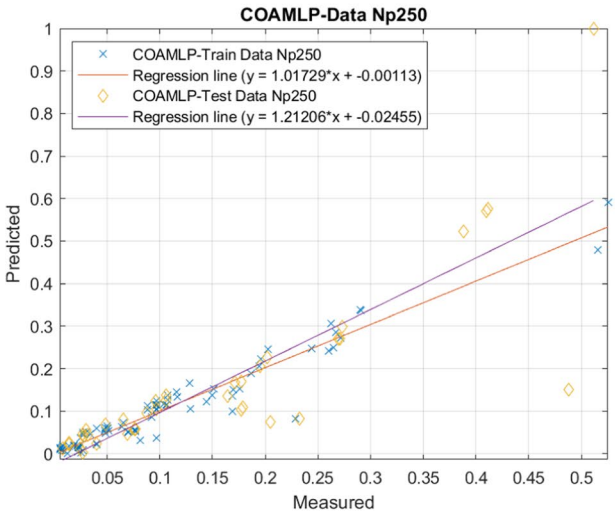

(e) COAMLP - N_p250

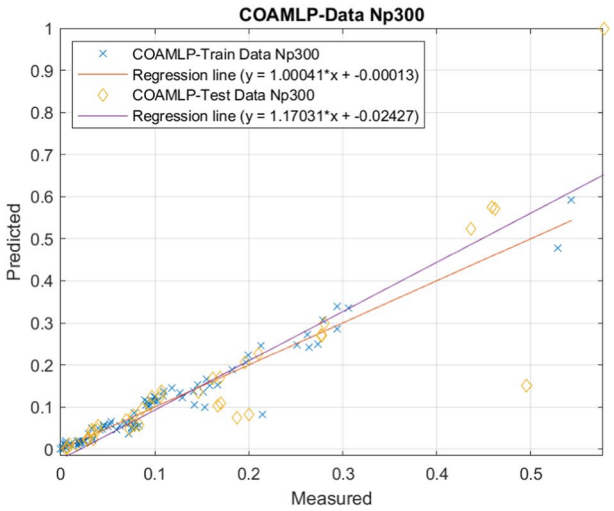

(f) COAMLP - N_p300

Fig. 10 Training and testing findings from many datasets recommended by COAMLP structures

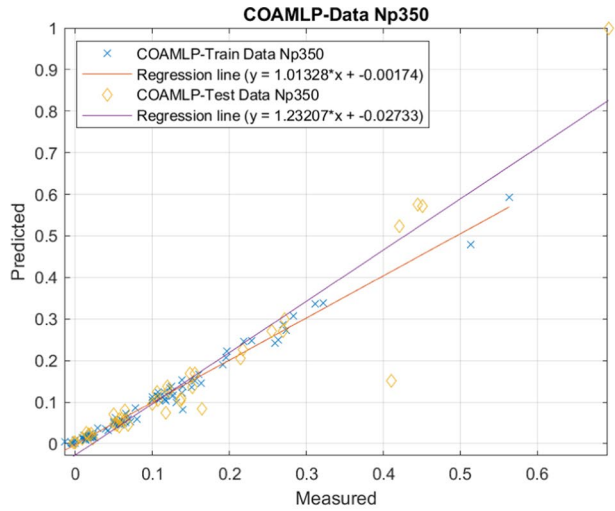

(g) COAMLP - N_p350

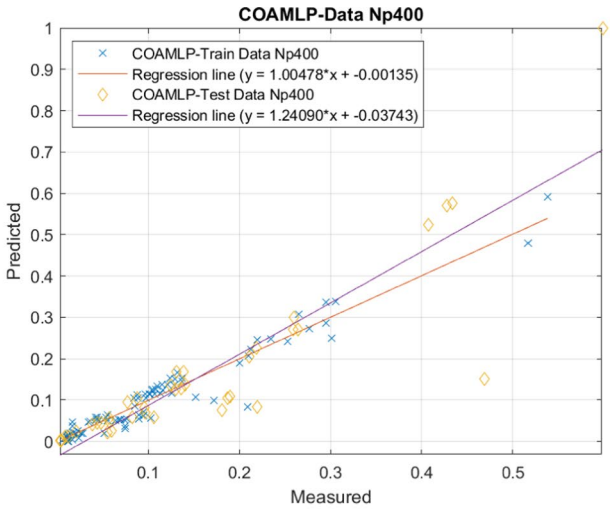

(h) COAMLP - N_p400

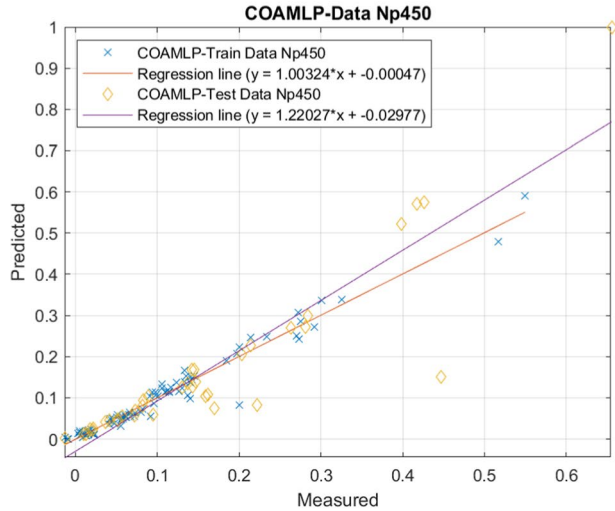

(i) COAMLP - N_p450

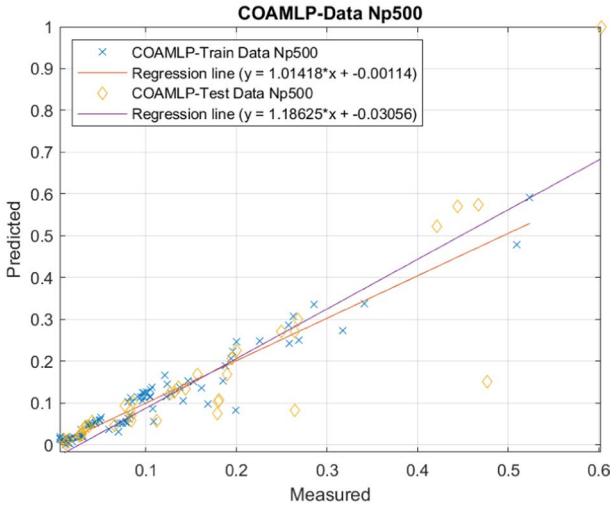

(j) COAMLP - N_p500

Fig. 10 (continued)

proposed network cases was good enough. Thus, using the ranking system, we could submit the final model to evaluate and forecast outcomes for fresh and unknown data.

Table 6 shows that for the training RMSE and R^2 databases, the hybrid's projected accuracy indices TLBO, MVO, COA, and ER-WCA models were (0.01012 and 0.99536), (0.01028 and 0.99522), (0.01336 and 0.9919), and (0.00611 and 0.9983), respectively. These models were then identified as (0.05216 and 0.9651), (0.0514 and 0.96613), (0.06662 and 0.94239), and (0.03698 and 0.98261) for the testing datasets, respectively. When statistical factors like Root Mean Squared Error (RMSE), Mean Absolute Error (MAE), and Coefficient of Determination (R^2) are taken into account, experimental findings for simulating the quality of groundwater show how the hybrid ER-WCA-ANN forecasting technique has a greater prediction accuracy. According to these results, by changing the MLP's computational variables, the metaheuristic algorithms may analyze the relationship between outputs and significant factors. Table 6 additionally tabulates overall ranking results, primarily generated from accuracy findings (model performances), with the proviso that the RMSE and R^2 results for the different recommended hybrid approaches are conducted based on changes in the model population size. The best TLBO, MVO, COA, and ER-WCA's estimated training and testing RMSEs and R^2 values are shown in Table 5. According to the results, the suggested ER-WCA-MLP-based neural network has a greater connection between testing and training datasets for production.

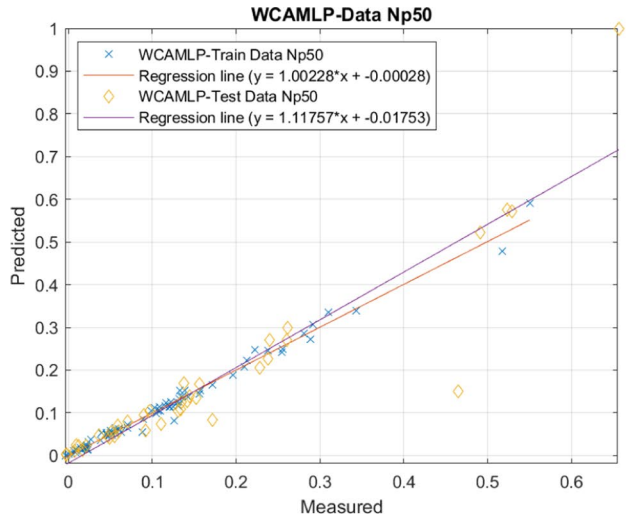

(a) ER-WCAMLP - N_p50

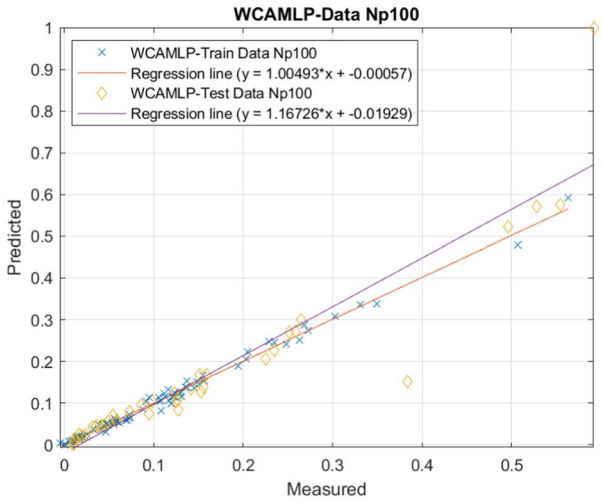

(b) ER-WCAMLP - N_p100

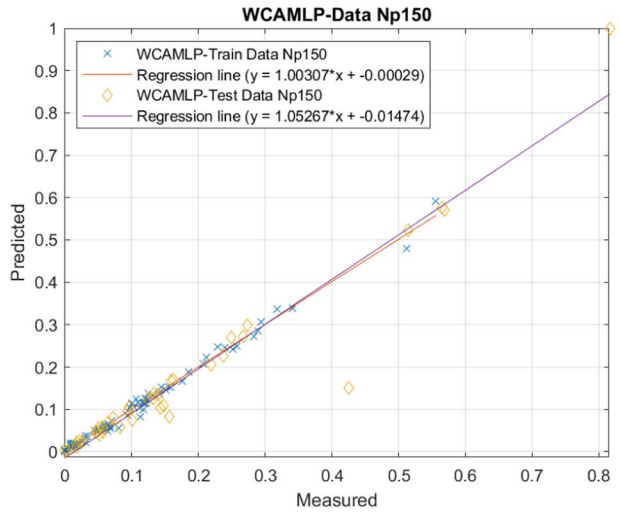

(c) ER-WCAMLP - N_p150

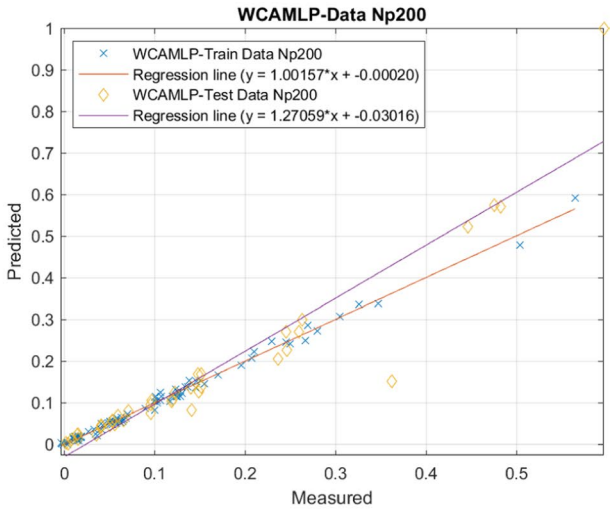

(d) ER-WCAMLP - N_p 200

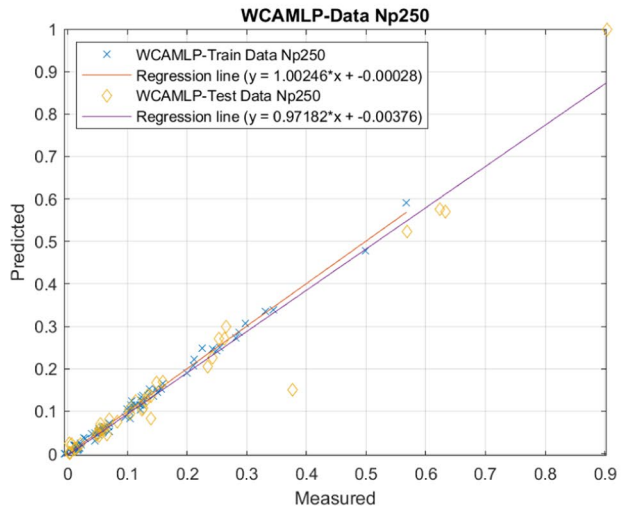

(e) ER-WCAMLP - N_p250

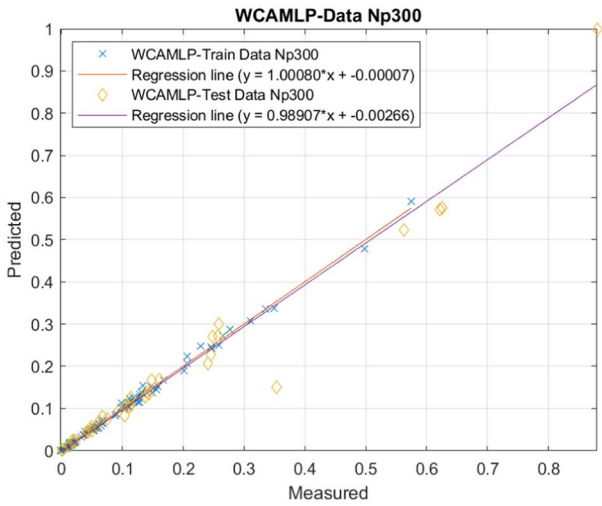

(f) ER-WCAMLP - N_p300

Fig. 11 Training and testing findings from many datasets recommended by WCAMLP structures

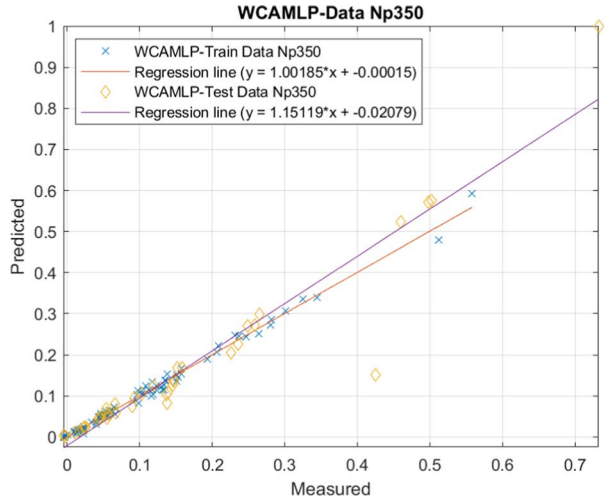

(g) ER-WCAMLP - N_p350

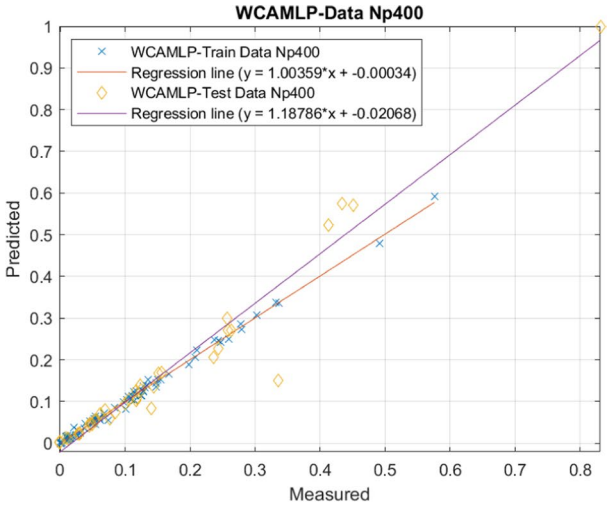

(h) ER-WCAMLP - N_p400

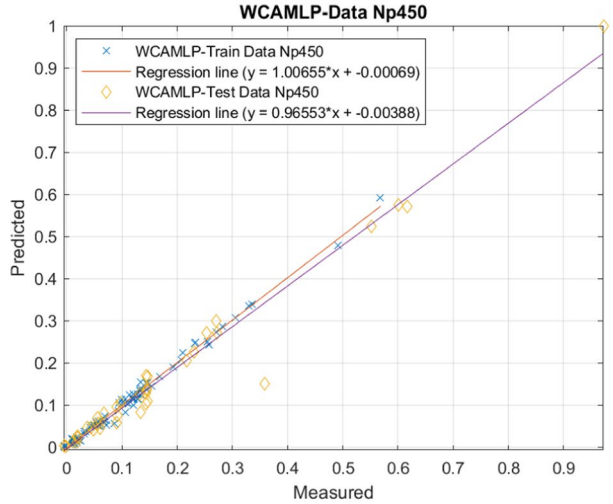

(i) ER-WCAMLP - N_p450

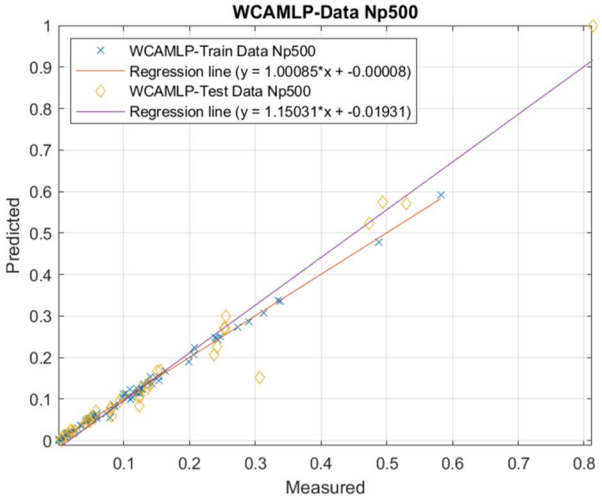

(j) ER-WCAMLP - N_p500

Fig. 11 (continued)

Conclusions

Using 540 samples taken at various periods across the Shiraz Plain, this research examined how well a variety of artificial intelligence systems performed in predicting the characteristics of one water quality parameter (Total hardness) in a groundwater flow system in a semi-arid environment. Three regressions based on neuronal evolution approaches were used with an ANN in this study to estimate the values of the dependent variables TH. The amounts of Na %, SO_4^{2-}, Cl, Na^+, Mg^{2+}, Ca^{2+}, HCO_3^-, K^+, and pH are seen as independent variables, and different ANN structures were built in order to provide a reliable solution. The effects of each setup were examined. It is possible to identify the best neural network-based model by using the nodes of each hidden layer. Four unique hybrid optimization methods, including the TLBO, MVO, COA, and ER-WCA, were created on the foundation of the optimized ANN structure. Evaluation measures (R^2, RMSE, MSE, and MAE) were used to all created models to assess their efficacy.

The estimated accuracy indices of the hybrid model for the training RMSE and R^2datasets TLBO, MVO, COA, and ER-WCA models were (0.01012 and 0.99536), (0.01028 and 0.99522), (0.01336 and 0.9919), and (0.00611 and 0.9983), respectively. These models were later found to be (0.05216 and 0.9651), (0.0514 and 0.96613), (0.06662 and 0.94239), and (0.03698 and 0.98261), respectively, for the testing datasets. With R^2 values of 0.9983 and 0.98261, and RMSE values of 0.03698 and 0.00611 in the training and testing datasets, respectively, the ER-WCAMLP technique (with a population size of 500 and eight neurons in each hidden

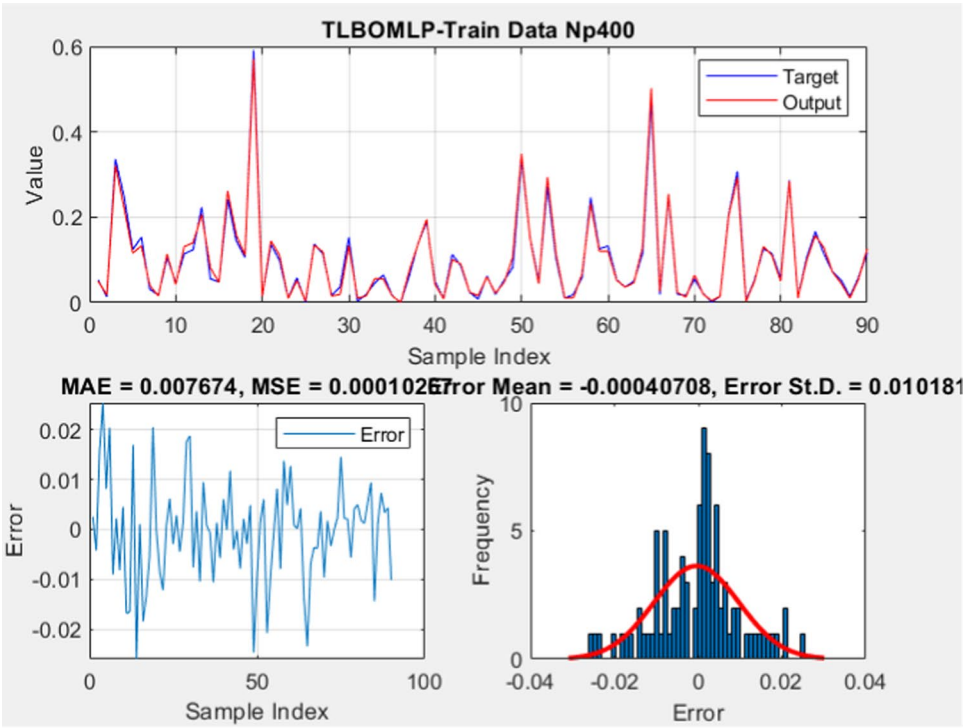

(a) TLBO 400-training

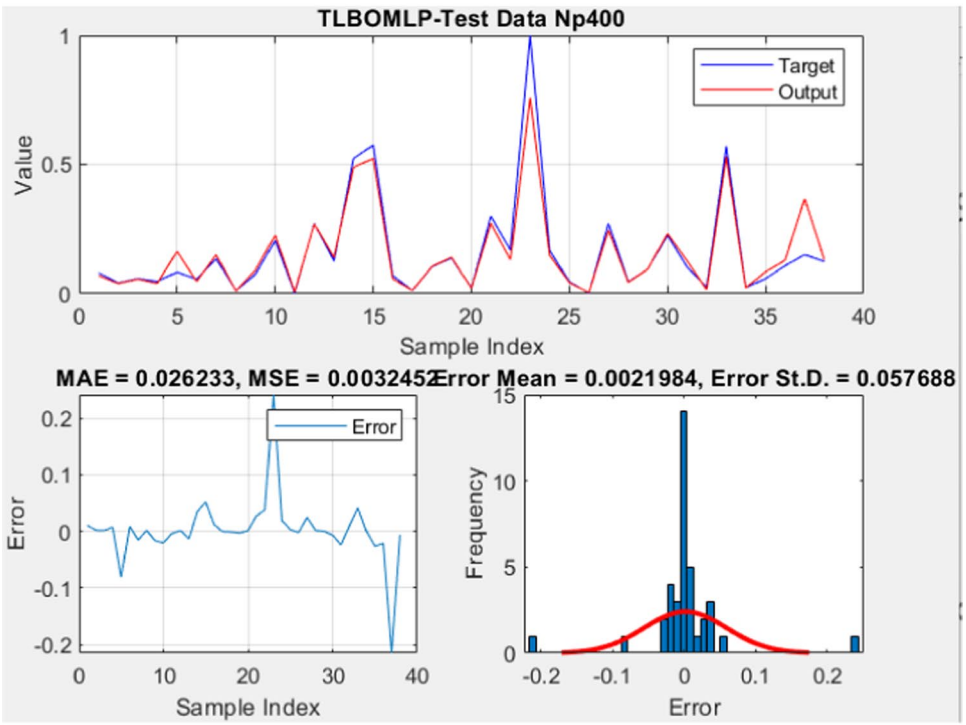

(b) TLBO 400-Testing

Fig. 12 The error and MAE frequency for the model suggested by TLBOMLP with the best match

layer) provided the most accurate prediction for the TH compared to all other developed models. Excellent accuracy of the network outputs (ER-WCA) generated by the created network from the training and test data set demonstrates that it is sufficiently reliable and may be utilized in the management of water resources in this particular groundwater flow

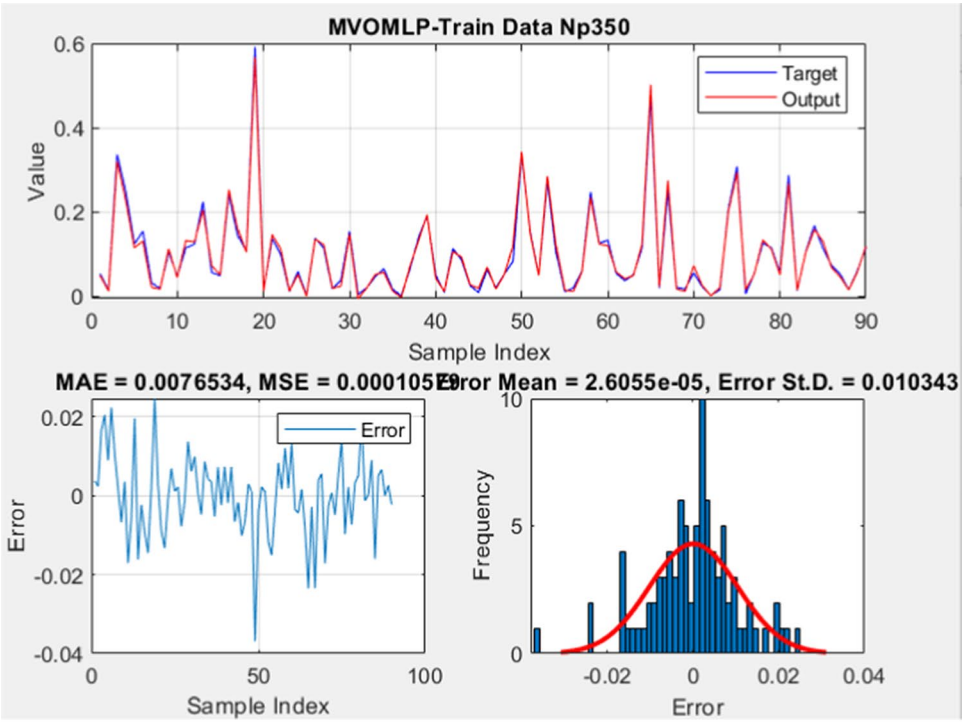

(a) MVOMLP 350-training

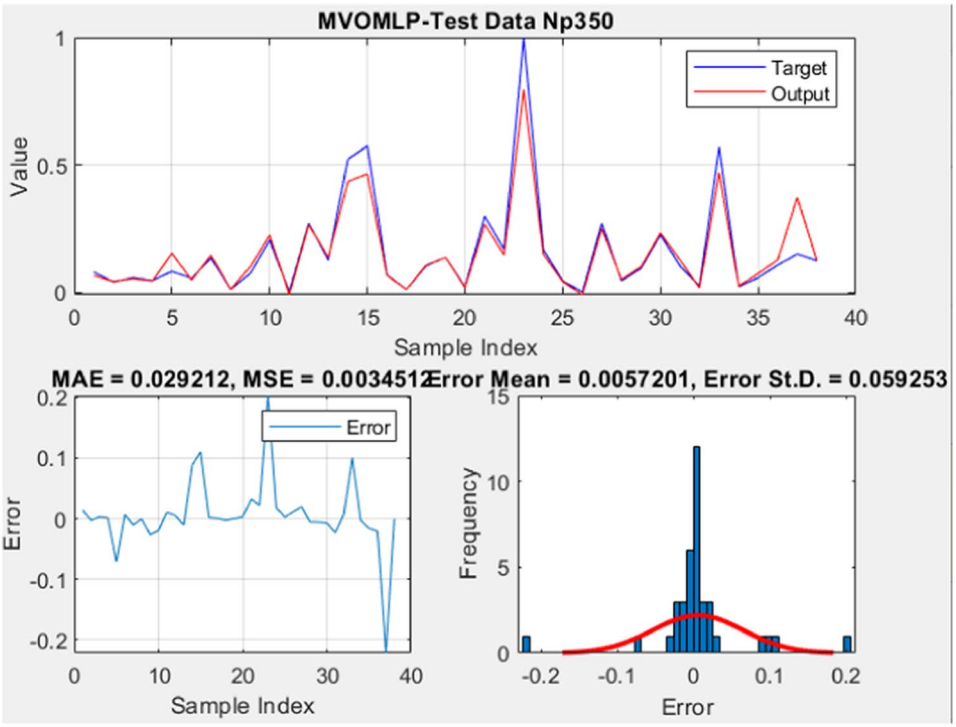

(b) MVOMLP 350-Testing

Fig. 13 The error and MAE frequency for the model suggested by MVOMLP with the best match

system, especially for upcoming groundwater quality assessments. The model may be considered to be a groundwater quality assessment tool that is novel.

The assessment indicated that ER-WCA-ANN yields more consistent results when compared to the target. In conclusion, it is essential to note that the high the results from the network's

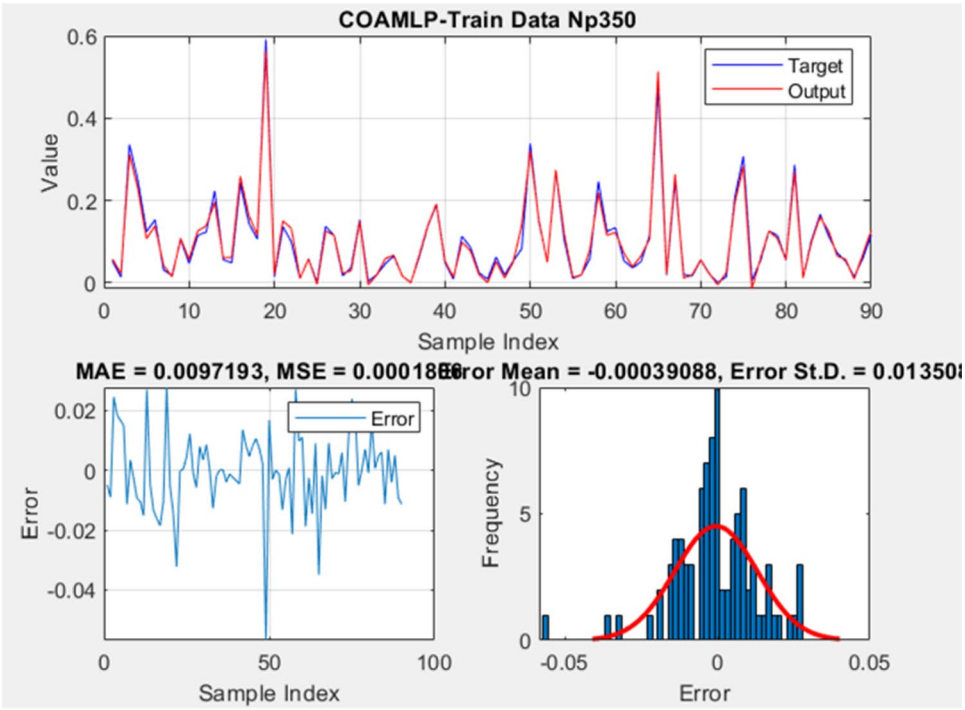

(a) COAMLP 350-training

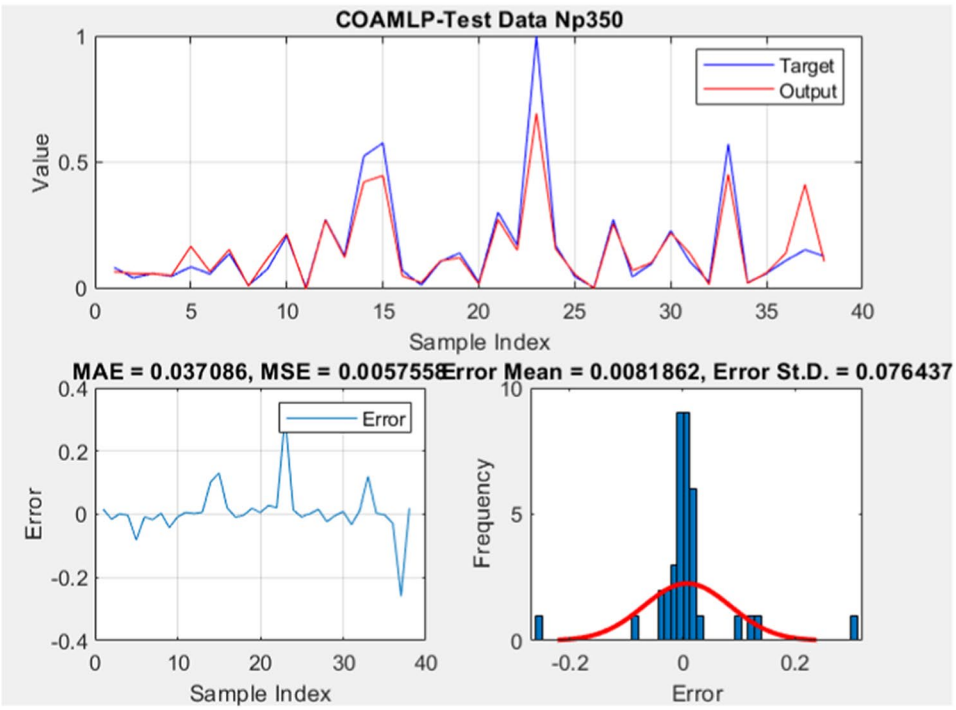

(b) COAMLP 350-Testing

Fig. 14 The error and MAE frequency for the model suggested by COAMLP with the best match

accuracy derived from the experimental data set demonstrates that all four expanded networks are sufficiently reliable and can be used in the future for assessing groundwater quality.

In addition, the ER-WCA model required a relatively short period of training. AI was used to determine the importance of the TH model over other expanded models for each

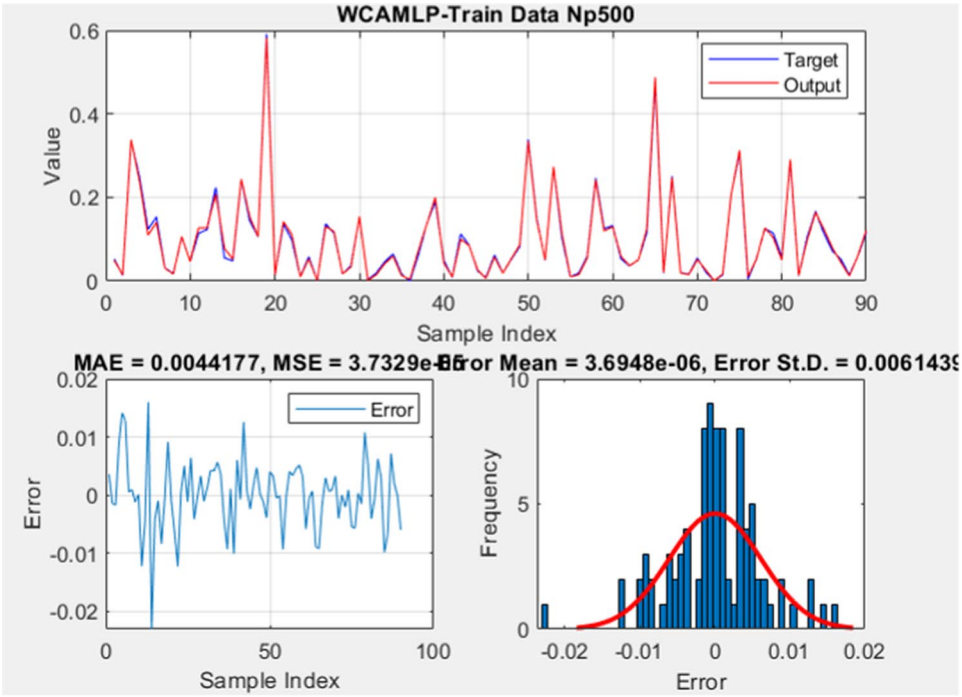

(a) ER-WCAMLP 500-training

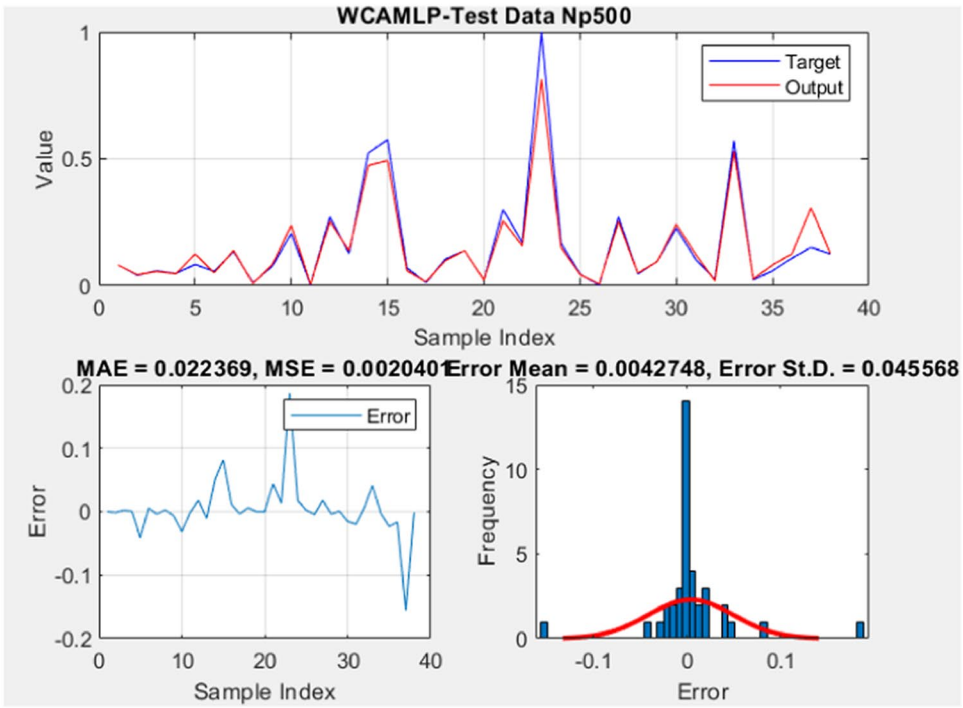

(b) ER-WCAMLP 500-Testing

Fig. 15 The error and MAE frequency for the model suggested by ER-WCAMLP with the best match

groundwater parameter by comparing the developed models. Due to their complexity, without the aid of computational tools, it is difficult to understand the hydrologic characteristics and status of groundwater systems. This work provides a thorough examination of the numerous AI approaches, techniques, and methodologies. The review of relevant literature

demonstrates that ANNs, ANFIS, EA, and SVM are effective and precise instruments for assessing and controlling the quality of groundwater. Additionally, combining appropriate machine learning techniques is much more successful than using them alone. As a result, AI modeling techniques can be utilized to design and plan pollution prevention and groundwater management strategies. The findings of this paper call for additional comparative studies of soft computing approaches employing data from other regions with distinct climatic conditions and data availability to bolster the conclusions reached.

Table 2 Network findings for several planned TLBOMLP swarm sizes based on two statistical metrics

Swarm size	Training dataset		Testing dataset		Scoring				Total score	Rank
	RMSE	R^2	RMSE	R^2	Training		Testing			
50	0.01849	0.9844	0.07228	0.93183	1	1	1	1	4	10
100	0.01078	0.9947	0.04257	0.97689	8	8	10	10	36	2
150	0.01537	0.9893	0.06725	0.94127	2	2	4	4	12	8
200	0.01337	0.9919	0.07115	0.93402	3	3	2	2	10	9
250	0.01115	0.9944	0.05968	0.95405	7	7	6	6	26	4
300	0.01222	0.9932	0.06053	0.9527	5	5	5	5	20	6
350	0.01049	0.9950	0.05534	0.96062	9	9	8	8	34	3
400	0.01012	0.9954	0.05216	0.9651	10	10	9	9	38	1
450	0.01181	0.9937	0.05965	0.95411	6	6	7	7	26	4
500	0.013	0.9923	0.06774	0.94039	4	4	3	3	14	7

Table 3 Network findings for several planned MVOMLP swarm sizes based on two statistical metrics

Swarm size	Training dataset		Testing dataset		Scoring				Total score	Rank
	RMSE	R^2	RMSE	R^2	Training		Testing			
50	0.01312	0.9922	0.07117	0.93398	5	5	2	2	14	9
100	0.01324	0.9920	0.06434	0.94638	4	4	4	4	16	7
150	0.01674	0.9873	0.05702	0.95814	1	1	8	8	18	5
200	0.01259	0.9928	0.08731	0.8988	7	7	1	1	16	7
250	0.01455	0.9904	0.05909	0.95498	2	2	7	7	18	5
300	0.01439	0.9906	0.06669	0.94228	3	3	3	3	12	10
350	0.01028	0.9952	0.0514	0.96613	9	9	10	10	38	1
400	0.01283	0.9925	0.06154	0.95106	6	6	6	6	24	4
450	0.01079	0.9947	0.05545	0.96046	8	8	9	9	34	2
500	0.00898	0.9964	0.06427	0.9465	10	10	5	5	30	3

Table 4 Network findings for several planned COAMLP swarm sizes based on two statistical metrics

Swarm size	Training dataset		Testing dataset		Scoring				Total score	Rank
	RMSE	R^2	RMSE	R^2	Training		Testing			
50	0.03039	0.9573	0.11645	0.81126	3	3	1	1	8	9
100	0.03414	0.9458	0.10079	0.86252	1	1	3	3	8	9
150	0.03109	0.9553	0.09941	0.86652	2	2	4	4	12	7
200	0.02184	0.9782	0.09709	0.87314	8	8	5	5	26	4
250	0.02725	0.9659	0.10852	0.83854	4	4	2	2	12	7
300	0.02298	0.9759	0.09528	0.87816	7	7	6	6	26	4
350	0.01336	0.9919	0.06662	0.94239	10	10	10	10	40	1
400	0.02555	0.9700	0.09266	0.88518	6	6	8	8	28	3
450	0.0199	0.9819	0.08358	0.90769	9	9	9	9	36	2
500	0.02583	0.9694	0.09413	0.88128	5	5	7	7	24	6

Table 5 Network findings for several planned EER-WCAMLP swarm sizes based on two statistical metrics

Swarm size	Training dataset		Testing dataset		Scoring				Total score	Rank
	RMSE	R^2	RMSE	R^2	Training		Testing			
50	0.01117	0.9943	0.07703	0.92218	1	1	1	1	4	10
100	0.00921	0.9962	0.07309	0.93024	4	3	2	2	11	9
150	0.00981	0.9956	0.05526	0.96074	2	2	5	5	14	7
200	0.00837	0.9968	0.06812	0.9397	6	6	3	3	18	6
250	0.00815	0.9970	0.04403	0.97525	7	7	7	7	28	3
300	0.00675	0.9979	0.04202	0.97749	9	9	8	8	34	2
350	0.00922	0.9962	0.06215	0.95007	3	3	4	4	14	7
400	0.00686	0.9979	0.04566	0.97337	8	8	6	6	28	3
450	0.00901	0.9963	0.03729	0.98232	5	5	9	9	28	3
500	0.00611	0.9983	0.03698	0.98261	10	10	10	10	40	1

Table 6 The performance of all four proposed methods using two statistical indices for network results

Method	Swarm size	Training dataset		Testing dataset		Scoring				Total score	Rank
		RMSE	R^2	RMSE	R^2	Training		Testing			
TLBOMLP	400	0.01012	0.99536	0.05216	0.9651	3	3	2	2	10	2
MVOMLP	350	0.01028	0.99522	0.0514	0.96613	2	2	3	3	10	2
COAMLP	350	0.01336	0.9919	0.06662	0.94239	1	1	1	1	4	4
ER-WCAMLP	500	0.00611	0.9983	0.03698	0.98261	4	4	4	4	16	1

Author contributions All authors contributed to the study's conception and design. HM: performed Material preparation and writing, reviewed, analyzed data, MS and AAD: Data collection, writing, reviewed, edited. SA-JA and HA: Revision preparation, writing and editing. All authors read and approved the final manuscript.

Funding No funding.

Data availability The data is available as per reader request.

Declarations

Conflict of interest The authors have no financial or proprietary interests in any material discussed in this article.

References

Abiodun OI, Jantan A, Omolara AE, Dada KV, Mohamed NA, Arshad H (2018) State-of-the-art in artificial neural network applications: a survey. Heliyon 4(11):e00938. https://doi.org/10.1016/j.heliyon.2018.e00938

Adnan Ikram RM, Khan I, Moayedi H, Ahmadi Dehrashid A, Elkhrachy I, Nguyen Le B (2023) Novel evolutionary-optimized neural network for predicting landslide susceptibility. Environ Dev Sustain 19:1–33.

Ahmadi Dehrashid A, Dong H, Fatahizadeh M, Gholizadeh Touchaei H, Gör M, Moayedi H, Salari M, Thi QT (2024) A new procedure for optimizing neural network using stochastic algorithms in predicting and assessing landslide risk in East Azerbaijan. Stoch Environ Res Risk Assess 1–30. https://doi.org/10.1007/s00477-024-02690-7

Almutairi K, Algarni S, Alqahtani T, Moayedi H, Mosavi A (2022) A TLBO-tuned neural processor for predicting heating load in residential buildings. Sustainability 14(10):5924

Alweshah M, Al-Sendah M, Dorgham OM, Al-Momani A, Tedmori S (2020) Improved water cycle algorithm with probabilistic neural network to solve classification problems. Clust Comput 23:2703–2718

Badeenezhad A, Tabatabaee HR, Nikbakht H-A, Radfard M, Abbasnia A, Baghapour MA, Alhamd M (2020) Estimation of the groundwater quality index and investigation of the affecting factors their changes in Shiraz drinking groundwater, Iran. Groundw Sustain Dev 11:100435

Bui DT, Pradhan B, Nampak H, Bui Q-T, Tran Q-A, Nguyen Q-P (2016) Hybrid artificial intelligence approach based on neural fuzzy inference model and metaheuristic optimization for flood susceptibilitgy modeling in a high-frequency tropical cyclone area using GIS. J Hydrol 540:317–330

Chen W, Panahi M, Khosravi K, Pourghasemi HR, Rezaie F, Parvinnezhad D (2019a) Spatial prediction of groundwater potentiality using ANFIS ensembled with teaching-learning-based and biogeography-based optimization. J Hydrol 572:435–448

Chen W, Shahabi H, Shirzadi A, Hong H, Akgun A, Tian Y, Liu J, Zhu A-X, Li S (2019b) Novel hybrid artificial intelligence approach of bivariate statistical-methods-based kernel logistic regression classifier for landslide susceptibility modeling. Bull Eng Geol Env 78:4397–4419

Coulibaly P, Anctil F, Bobée B (1999) Prévision hydrologique par réseaux de neurones artificiels: état de l'art. Can J Civ Eng 26(3):293–304

David S (1993) The Water Cycle (John Yates, Illus). Thomson Learning, New York

Eskandar H, Sadollah A, Bahreininejad A, Lumpur K (2013) Weight optimization of truss structures using water cycle algorithm. Int J Optim Civ Eng 3(1):115–129

Feindt M, Kerzel U (2006) The NeuroBayes neural network package. Nucl Instrum Methods Phys Res Sect A Acceler Spectrom Detect Assoc Equip 559(1):190–194. https://doi.org/10.1016/j.nima.2005.11.166

Foong LK, Moayedi H, Lyu Z (2021) Computational modification of neural systems using a novel stochastic search scheme, namely evaporation rate-based water cycle algorithm: an application in geotechnical issues. Eng Comput 37:3347–3358

Gholami V, Booij M (2022) Use of machine learning and geographical information system to predict nitrate concentration in an unconfined aquifer in Iran. J Clean Prod 360:131847

Hagan MT, Demuth HB, Beale M (1997) Neural network design. PWS Publishing Co.

Hanoon MS, Ammar AM, Ahmed AN, Razzaq A, Birima AH, Kumar P, Sherif M, Sefelnasr A, El-Shafie A (2022) Application of soft computing in predicting groundwater quality parameters. Front Environ Sci 10:12

Hudcovic T (2022) TLBO-based algorithms for minimalization of multi-ray path lengths in voxel object representations on the GPU

Hussien AG, Hashim FA, Qaddoura R, Abualigah L, Pop A (2022) An enhanced evaporation rate water-cycle algorithm for global optimization. Processes 10(11):2254

Ikram RM, Dehrashid AA, Zhang B, Chen Z, Le BN, Moayedi H (2023) A novel swarm intelligence: cuckoo optimization algorithm (COA) and SailFish optimizer (SFO) in landslide susceptibility assessment. Stochastic Environ Res Risk Assessment 37(5):1717–1743

Khalid S, Shahid M, Natasha, Shah AH, Saeed F, Ali M, Qaisrani SA, Dumat C (2020) Heavy metal contamination and exposure risk assessment via drinking groundwater in Vehari, Pakistan. Environ Sci Pollut Res 27:39852–39864

Khashei-Siuki A, Kouchkzadeh M, Ghahraman B (2011) Predicting dryland wheat yield from meteorological data using expert system, Khorasan Province, Iran. J Agric Sci Technol 13(4):627–640

Khosravi K, Panahi M, Tien Bui D (2018) Spatial prediction of groundwater spring potential mapping based on an adaptive neuro-fuzzy inference system and metaheuristic optimization. Hydrol Earth Syst Sci 22(9):4771–4792

Khudair BH, Jasim MM, Alsaqqar AS (2018) Artificial neural network model for the prediction of groundwater quality. Civ Eng J 4(12):2959–2970

Leal Filho W, Barbir J, Sima M, Kalbus A, Nagy GJ, Paletta A, Villamizar A, Martinez R, Azeiteiro UM, Pereira MJ (2020) Reviewing the role of ecosystems services in the sustainability of the urban environment: a multi-country analysis. J Clean Prod 262:121338

Mirjalili S, Mirjalili SM, Hatamlou A (2016) Multi-verse optimizer: a nature-inspired algorithm for global optimization. Neural Comput Appl 27(2):495–513

Moayedi H, Mosavi A (2021) Hybridizing neural network with multi-verse, black hole, and shuffled complex evolution optimizer algorithms predicting the dissolved oxygen

Moayedi H, Canatalay PJ, Ahmadi Dehrashid A, Cifci MA, Salari M, Le BN (2023a) Multilayer perceptron and their comparison with two nature-inspired hybrid techniques of biogeography-based optimization (BBO) and backtracking search algorithm (BSA) for assessment of landslide susceptibility. Land 12(1):242

Moayedi H, Salari M, Dehrashid AA, Le BN (2023b) Groundwater quality evaluation using hybrid model of the multi-layer perceptron combined with neural-evolutionary regression techniques: case study of Shiraz plain. Stoch Environ Res Risk Assess 37:1–16

Moayedi H, Ahmadi Dehrashid A, Nguyen Le B (2024) A novel problem-solving method by multi-computational optimisation of artificial neural network for modelling and prediction of the flow erosion processes. Eng Appl Comput Fluid Mech 31;18(1):2300456

Naghibi SA, Pourghasemi HR, Dixon B (2016) GIS-based groundwater potential mapping using boosted regression tree, classification and regression tree, and random forest machine learning models in Iran. Environ Monit Assess 188:1–27

Naghibi SA, Ahmadi K, Daneshi A (2017) Application of support vector machine, random forest, and genetic algorithm optimized random forest models in groundwater potential mapping. Water Resour Manage 31:2761–2775

Nordin NFC, Mohd NS, Koting S, Ismail Z, Sherif M, El-Shafie A (2021) Groundwater quality forecasting modelling using artificial intelligence: a review. Groundw Sustain Dev 14:100643

Organization WH (1993) The ICD-10 classification of mental and behavioural disorders: diagnostic criteria for research, vol 2. World Health Organization, Geneva

Prakash N, Manconi A, Loew S (2021) A new strategy to map landslides with a generalized convolutional neural network. Sci Rep 11(1):9722. https://doi.org/10.1038/s41598-021-89015-8

Rahmati O, Pourghasemi HR, Melesse AM (2016) Application of GIS-based data driven random forest and maximum entropy models for groundwater potential mapping: a case study at Mehran Region, Iran. CATENA 137:360–372

Rajabioun R (2011) Cuckoo Optimization Algorithm. Appl Soft Comput 11(8):5508–5518

Rakhshandehroo GR, Vaghefi M, Aghbolaghi MA (2012) Forecasting groundwater level in Shiraz plain using artificial neural networks. Arab J Sci Eng 37:1871–1883

Rao RV, Savsani VJ, Vakharia D (2011) Teaching–learning-based optimization: a novel method for constrained mechanical design optimization problems. Comput Aid Des 43(3):303–315

Sadollah A, Eskandar H, Bahreininejad A, Kim JH (2015) Water cycle algorithm with evaporation rate for solving constrained and unconstrained optimization problems. Appl Soft Comput 30:58–71

Sadollah A, Eskandar H, Lee HM, Kim JH (2016) Water cycle algorithm: a detailed standard code. SoftwareX 5:37–43

Salami E, Ehetshami M, Karimi-Jashni A, Salari M, Nikbakht Sheibani S, Ehteshami A (2016a) A mathematical method and artificial neural network modeling to simulate osmosis membrane's performance. Model Earth Syst Environ 2:1–11

Salami E, Salari M, Ehteshami M, Bidokhti N, Ghadimi H (2016b) Application of artificial neural networks and mathematical modeling for the prediction of water quality variables (case study: southwest of Iran). Desalin Water Treat 57(56):27073–27084

Salari M, Rakhshandehroo G, Ehetshami M (2017) Investigating the spatial variability of some important groundwater quality factors based on the geostatistical simulation (case study: Shiraz plain). Desalin Water Treat 65(2):163–174

Salari M, Shahid ES, Afzali SH, Ehteshami M, Conti GO, Derakhshan Z, Sheibani SN (2018) Quality assessment and artificial neural networks modeling for characterization of chemical and physical parameters of potable water. Food Chem Toxicol 118:212–219

Salari S, Moghaddasi M, Mohammadi Ghaleni M, Akbari M (2021) Groundwater level prediction in Golpayegan aquifer using ANFIS and PSO combination. Iran J Soil Water Res 52(3):721–732

Sarker B, Keya KN, Mahir FI, Nahiun KM, Shahida S, Khan RA (2021) Surface and ground water pollution: Causes and effects of urbanization and industrialization in South Asia. Sci Rev 7(3):32–41

Shen Y, Ahmadi Dehrashid A, Bahar RA, Moayedi H, Nasrollahizadeh B (2023) A novel evolutionary combination of artificial intelligence algorithm and machine learning for landslide susceptibility mapping in the west of Iran. Environ Sci Pollut Res 30(59):123527–123555

Sunayana KK, Dube O, Sharma R (2020) Use of neural networks and spatial interpolation to predict groundwater quality. Environ Dev Sustain 22(4):2801–2816

Tsakiri K, Marsellos A, Kapetanakis S (2018) Artificial neural network and multiple linear regression for flood prediction in Mohawk River, New York. Water 10(9):1158

Tyralis H, Papacharalampous G, Langousis A (2019) A brief review of random forests for water scientists and practitioners and their recent history in water resources. Water 11(5):910

Wang S-C (2003) Artificial neural network. In: Wang S-C (ed) Interdisciplinary computing in Java programming. Springer, New York, pp 81–100. https://doi.org/10.1007/978-1-4615-0377-4_5

Wu Z, Moayedi H, Salari M, Le BN, Ahmadi Dehrashid A (2024) Assessment of sodium adsorption ratio (SAR) in groundwater: Integrating experimental data with cutting-edge swarm intelligence approaches. Stochastic Environ Res Risk Assess 1-18

Yalcintas M, Akkurt S (2005) Artificial neural networks applications in building energy predictions and a case study for tropical climates. Int J Energy Res 29(10):891–901

Yang X-S, Deb S (2009) Cuckoo search via Lévy flights. In: 2009 World congress on nature & biologically inspired computing (NaBIC)

Zhu M, Wang J, Yang X, Zhang Y, Zhang L, Ren H, Wu B, Ye L (2022) A review of the application of machine learning in water quality evaluation. Eco-Environ Health 1:107

Zurada J (1992) Introduction to artificial neural systems. West Publishing Co., Eagan